Universidad de Concepción
Facultad de Ciencias Físicas y Matemáticas
Ciencias Físicas

Dipole-dipole Interactions through a Lens

Thesis to opt for the degree of Master of Science with mention in Physics

by

Aníbal Luciano Olivera Morales

Thesis Director : Dr. Pablo Solano

Comisión : Dr. Aldo Delgado
Dra. Carla Hermann
Dr. Stephen Walborn
Director del programa

CONCEPCIÓN • CHILE
MARZO 2022

Table of Contents

A mi madre.

otro ya recibió en otras borrosas
tardes los muchos libros y la sombra.

Poema de los dones
Jorge Luis Borges, *El hacedor*.

Agradecimientos

.

Gracias a mi familia, la rara. Gracias a mis amigos del colegio, por forzarnos a pensar. Gracias a La Daniela, la única La daniela. Gracias a mis amigos de la Universidad, por dispensar su juventud aquí.

.

Gracias al Averno, al Chef, a La Bodeguita (énfasis), a los pastos, a la Biblioteca, a algunas plazas.

.

Gracias a Los Jaivas, Fito Páez, el Flaco, La Máquina, el Macha, Congreso, Miles Davis, Trioscapes, Larrea Trip.

.

Gracias profesores, los grandes, gracias Carla, en especial gracias Pablo.

Abstract

In the present work, the interactions mediated by fluctuations between two atoms in the presence of an aplanatic lens were studied, demonstrating an improvement in their resonant dipole-dipole interaction. We derive the field propagation of the linear optical system in terms of the dyadic Green's tensor for an aplanatic lens. The collective atomic dynamics is analyzed via a Lindblad master equation for open systems, which allows characterizing the dispersive and dissipative interactions between distant atoms, and also through their respective interaction Hamiltonian. Thus, it is shown that the resonant dipole-dipole coupling between atoms can be enhanced in the focal zone of the lens, enough to guarantee an atomic trap with a reasonable lifetime. Our work opens new avenues to expand dipole-dipole interactions to macroscopic scales and the experimental platforms to study them.

Resumen

En el presente trabajo se estudiaron las interacciones mediadas por las fluctuaciones de los campos entre dos átomos en presencia de una lente aplanática, demostrando un aumento en su interacción resonante dipolo-dipolo. Derivamos la propagación del campo a través del sistema óptico lineal en términos del tensor de Green diádico para tal lente con ambas distancias focales iguales. La dinámica colectiva es analizada a través de la ecuación maestra de Lindblad para sistemas abiertos, la cual permite caracterizar las interacciones dispersivas y disipativas entre átomos distantes, y a también mediante su respectivo Hamiltoniano de interacción. Así, se demuestra que el acoplamiento dipolo-dipolo resonante entre los átomos la zona focal se puede aumentar significativamente, lo suficiente como para garantizar una trampa atómica con un tiempo de vida tiempo razonable. Nuestro trabajo abre nuevas vías para expandir las interacciones dipolo-dipolo a escalas macroscópicas y añade una plataforma experimental para estudiarlas.

Chapter 1

Introduction

Quantum electrodynamics (QED) has the fundamental and fascinating feature that quantum fluctuations can result in forces between two neutral bodies, known as fluctuation forces [1, 2]. In the context of atomic interactions these forces are typically referred to as Casimir-Polder, or van der Waals forces [3]. While typically weak, these forces become relevant in nanophotonic systems. For example, the Casimir-Polder forces on atoms are detrimental for trapping particles near surfaces [4]. This fluctuation-mediated forces can be engineered in different ways, for example, by modifying properties of external macroscopic bodies [5–9], the density of modes of the electromagnetic (EM) field via the geometry [10], using magnetic interactions [11], driving the system [4,12], or preparing the system in a collective state [13].

The control of individual atoms by high numerical aperture (NA) lenses, which collect and focus light into small regions, has reached sufficient development to explore atom-field interactions, such as quantum gases microscopes [14], programmable atom arrays [15, 16], and other novel arrangements of lenses [17, 18]. An important achievement of this control of single nano-particles was to reveal the dynamics of the proteins in our own DNA using optical tweezers [19]. State-of-the-art optical elements allow for a NA as high as 0.92 [20], near the theoretical limit. In the context of high-NA lenses, the possibility of studying long-range atom-atom interactions, not yet explored, opens up.

The possibility of guiding a fraction of an emitter's light over long distances has been of significant interest in waveguide quantum electrodynamics. This branch

rely on the evanescent light-matter coupling wherein the emitters are either placed nearby a solid waveguide structure.

In the literature it is usual to find long-range interaction between atom by guiding a fraction of the light from an emitter over macroscopic distances. This has been of significant interest in the quantum electrodynamic waveguide branch, which rely on the evanescent light-matter coupling wherein the emitters are either placed nearby a solid waveguide structure in order to establish a collective state between the particles [21–24]. On the other hand, imaging systems imply large operating distances that allow atoms to be treated as if they were in free space [25], while facilitating interactions with their distant counterparts. The possibility of enhancing the long-range interaction using the far-field emission represents an exciting way to combine the collective behavior with the exchange of real photons.

In this work we explore the idea of using an ideal lens together with a weak external drive to amplify and engineer the interaction between two distant atoms. As the atoms scatter the laser field, the lens collects and amplifies the far-field resonant dipole-dipole interaction mediated via the drive photons. This opens the possibility of using atomic imaging technology for engineering long-range dipole-dipole interactions and implementing collective systems without near-field interactions.

Chapter 2

Theoretical Foundations

As humans, we like light. We look forward to the arrival of spring and summer, which are characterized by a greater presence of natural light for a longer time. This is mainly due to the fact that the energy of light quanta (photons) is within the energy range of electronic transitions in matter and, for evolutionary reasons, our eyes are adapted to detect this range (optical spectrum). This gives us the beauty of color.

The understanding of this moving phenomenon (light-matter interaction) has been one of the greatest advances in recent centuries. Thanks to this advance we can handle physical events as we please, something dreamed of by the 10,000 generations prior to ours. For the study of the interaction of an atom with radiation of different types, it will be convenient to have an idea of the relevant knowledge of the description of light, atoms, and the interaction between them.

With the beginning of the development of quantum mechanics came a revolutionary paradigm shift: light could be treated both as a wave and as a particle. Convention today dictates that light behaves as light or as a particle depending on which feature you exploit in your particular experiment. To describe optical radiation in nano-optics it is mostly sufficient to adopt the wave picture. This allows us to use classical field theory based on Maxwell's equations. Also, in nano-optics, the systems with which the light fields interact are small, such as individual molecules or single atoms, which requires a quantum description of the properties of the material. Therefore, in most cases we can use the framework of semi-classical theory, which

combines the classical picture of fields and the quantum picture of matter.

2.1 Electrodynamics

In 1873, James Clerk Maxwell combine the laws formerly established by Faraday, Ampère, Gauss, Poisson, and others and derived what would become the first equations for the dynamics of the electromagnetic field. Those corresponded to a macroscopic electrodynamics, considering charge densities ρ and current densities $\mathbf{j}$. In differential form and in SI units, Maxwell's macroscopic equations have the form

$$\nabla \cdot \mathbf{D}(\mathbf{r}, t) = \rho(\mathbf{r}, t) \tag{2.1.1}$$

$$\nabla \times \mathbf{E}(\mathbf{r}, t) = -\frac{\partial \mathbf{B}(\mathbf{r}, t)}{\partial t} \tag{2.1.2}$$

$$\nabla \cdot \mathbf{B}(\mathbf{r}, t) = 0 \tag{2.1.3}$$

$$\nabla \times \mathbf{H}(\mathbf{r}, t) = \frac{\partial \mathbf{D}(\mathbf{r}, t)}{\partial t} + \mathbf{j}(\mathbf{r}, t) \tag{2.1.4}$$

where $\mathbf{E}$ denotes the electric field, D the electric displacement, $\mathbf{H}$ the magnetic field, $\mathbf{B}$ the magnetic induction, $\mathbf{j}$ the current density, and ρ the charge density. These equations determine the behavior of fields. Centuries ago, the usual observable was force, and these fields came to explain strange phenomena such as "forces at a distance". The source terms in this description are continuous and macroscopic.

An important feature is the conservation of current, which is implicitly contained in Maxwell's equations. Taking the divergence of Eq. 2.1.4, using $\nabla \cdot \nabla \times \mathbf{H} = 0$, and and substituting Eq. 2.1.1 for $\nabla \cdot \mathbf{D}$ one obtains the continuity equation

$$\nabla \cdot \mathbf{j}(\mathbf{r}, t) + \frac{\partial \rho(\mathbf{r}, t)}{\partial t} = 0. \tag{2.1.5}$$

In a medium, the electromagnetic properties are most commonly discussed in terms

of the macroscopic polarization $\mathbf{P}$ and magnetization $\mathbf{M}$ according to

$$\mathbf{D}(\mathbf{r},t) = \epsilon_0 \mathbf{E}(\mathbf{r},t) + \mathbf{P}(\mathbf{r},t) \tag{2.1.6}$$

$$\mathbf{H}(\mathbf{r},t) = \frac{1}{\mu_0}\mathbf{B}(\mathbf{r},t) - \mathbf{M}(\mathbf{r},t) \tag{2.1.7}$$

where ϵ_0 and μ_0 are the permittivity and the permeability of vacuum, respectively. These equations do not impose any conditions on the medium and are therefore always valid. Substituting these relations in the Maxwells's Eqs. 2.1.2 and 2.1.4 we can obtain the inhomogeneous wave equations

$$\nabla \times \nabla \times \mathbf{E} + \frac{1}{c^2}\frac{\partial^2 \mathbf{E}}{\partial t^2} = -\mu_0 \frac{\partial}{\partial t}\left(\mathbf{j} + \frac{\partial \mathbf{P}}{\partial t} + \nabla \times \mathbf{M}\right) \tag{2.1.8}$$

$$\nabla \times \nabla \times \mathbf{H} + \frac{1}{c^2}\frac{\partial^2 \mathbf{H}}{\partial t^2} = \nabla \times \mathbf{j} + \nabla \times \frac{\partial \mathbf{P}}{\partial t} - \frac{1}{c^2}\frac{\partial^2 \mathbf{M}}{\partial t^2} \tag{2.1.9}$$

In a source-free vacuum we will obtain a wave equation for the fields $\mathbf{E}$ and $\mathbf{H}$, so it is straightforward to interpret

$$c = \frac{1}{\sqrt{\epsilon_0 \mu_0}} \tag{2.1.10}$$

as the vacuum speed of light. Equations 2.1.8 and 2.1.9 only dictate the behavior of the fields and do not impose any conditions on the medium considered, so they are universally valid. We can separate the current density term according to its origin, $\mathbf{j} = \mathbf{j}_s + \mathbf{j}_c$. The terms $\mathbf{j}_s$ and $\mathbf{j}_c$ are recognized as the source and induced conduction current density, respectively. Furthermore, to describe how matter behaves under these fields we need material equations known as constitutive relations

$$\mathbf{P}(\mathbf{r},t) = \epsilon_0 \chi_\mathrm{e} \mathbf{E}(\mathbf{r},t), \tag{2.1.11}$$

$$\mathbf{M}(\mathbf{r},t) = \chi_\mathrm{m} \mathbf{H}(\mathbf{r},t), \tag{2.1.12}$$

$$\mathbf{j}(\mathbf{r},t)_c = \sigma \mathbf{E}(\mathbf{r},t). \tag{2.1.13}$$

where σ is the electrical conductivity, and χ_e and χ_m denote the electric and magnetic susceptibility, respectively. Substituting these relations into the Eqs. 2.1.6 and

2.1.7 we can write

$$\mathbf{D}(\mathbf{r},t) = \epsilon_0 \epsilon_\mathrm{r} \mathbf{E}(\mathbf{r},t) \tag{2.1.14}$$

$$\mathbf{B}(\mathbf{r},t) = \mu_0 \mu_\mathrm{r} \mathbf{H}(\mathbf{r},t) \tag{2.1.15}$$

with $\epsilon_\mathrm{r} = \epsilon/\epsilon_0 = 1 + \chi_\mathrm{e}$ denoting the relative electric susceptibility, being ϵ the medium electric susceptibility, and $\mu_\mathrm{r} = \mu/\mu_0 = 1 + \chi_\mathrm{m}$ the relative magnetic susceptibility, where μ is the medium magnetic susceptibility.

An important fact to note is that electric and magnetic fields can be written in terms of a vector potential $\mathbf{A}$ and a scalar potential ϕ, defined by

$$\mathbf{E}(\mathbf{r},t) = -\frac{\partial}{\partial t}\mathbf{A}(\mathbf{r},t) - \nabla\phi(\mathbf{r},t) \tag{2.1.16}$$

$$\mathbf{B}(\mathbf{r},t) = \nabla \times \mathbf{A}(\mathbf{r},t). \tag{2.1.17}$$

They satisfy Maxwell's equations. Nevertheless, the potentials $\mathbf{A}$ and ϕ are not uniquely defined by Eqs. 2.1.16 and 2.1.17. This is caused by the freedom of gauge, i.e. if the potentials are replaced by new potentials $\tilde{\mathbf{A}}$ and $\tilde{\phi}$ according to

$$\mathbf{A} \rightarrow \tilde{\mathbf{A}} + \nabla\chi \tag{2.1.18}$$

$$\phi \rightarrow \tilde{\phi} - \partial\chi/\partial t \tag{2.1.19}$$

with $\chi(\mathbf{r},t)$ being an arbitrary gauge function, then Maxwell's equations remain unaffected. This is easily seen by introducing the above substitutions into the definitions of $\mathbf{A}$ and ϕ, Eqs. 2.1.16 and 2.1.17. This redundancy gives the freedom to choose a suitable gauge fixing according to what is convenient for each case.

It is generally more interesting to study the spectrum $\hat{\mathbf{E}}(\mathbf{r},\omega)$ of a time-dependent field $\mathbf{E}(\mathbf{r},t)$, which are related by the Fourier transform

$$\hat{\mathbf{E}}(\mathbf{r},\omega) = \frac{1}{2\pi}\int_{-\infty}^{\infty} \mathbf{E}(\mathbf{r},t)\mathrm{e}^{\mathrm{i}\omega t}\,\mathrm{d}t. \tag{2.1.20}$$

If we apply the Fourier transform to Maxwell's equations 2.1.1-2.1.4, we will get

$$\nabla \cdot \hat{\mathbf{D}}(\mathbf{r},\omega) = \hat{\rho}(\mathbf{r},\omega), \tag{2.1.21}$$

$$\nabla \times \hat{\mathbf{E}}(\mathbf{r},\omega) = \mathrm{i}\omega\hat{\mathbf{B}}(\mathbf{r},\omega), \tag{2.1.22}$$

$$\nabla \cdot \hat{\mathbf{B}}(\mathbf{r},\omega) = 0, \tag{2.1.23}$$

$$\nabla \times \hat{\mathbf{H}}(\mathbf{r},\omega) = -\mathrm{i}\omega\hat{\mathbf{D}}(\mathbf{r},\omega) + \hat{\mathbf{j}}(\mathbf{r},\omega). \tag{2.1.24}$$

The general time dependence is obtained from the inverse transform. For the rest of the text, $\hat{\mathbf{E}}(\mathbf{r},\omega) \equiv \mathbf{E}(\mathbf{r})$ will be used. Applying the operator $\nabla \times \frac{1}{\mu}$ to the Eq. 2.1.22, and using Eqs. 2.1.15, 2.1.14 and 2.1.24, we can write

$$\nabla \times \frac{1}{\mu}\nabla \times \mathbf{E}(\mathbf{r}) = \mathrm{i}\omega\nabla \times \frac{1}{\mu}\mathbf{B}(\mathbf{r}) \tag{2.1.25}$$

$$= \omega^2\epsilon\mathbf{E}(\mathbf{r}) + \mathrm{i}\omega\mathbf{j}_c(\mathbf{r}) + \mathrm{i}\omega\mathbf{j}_s(\mathbf{r}) \tag{2.1.26}$$

and finally, from the constitutive relation Eq. 2.1.13 we arrive to

$$\nabla \times \frac{1}{\mu}\nabla \times \mathbf{E}(\mathbf{r}) - \frac{\omega^2}{c^2}\left[\epsilon + \mathrm{i}\sigma/\left(\omega\epsilon_0\right)\right]\mathbf{E}(\mathbf{r}) = \mathrm{i}\omega\mu_0\mathbf{j}_s(\mathbf{r}) \tag{2.1.27}$$

$$\longrightarrow \qquad \nabla \times \nabla \times \mathbf{E}(\mathbf{r}) - k^2\mathbf{E}(\mathbf{r}) = \mathrm{i}\omega\mu_0\mu\mathbf{j}_s(\mathbf{r}) \tag{2.1.28}$$

where we replace the expression in brackets on the left-hand side of the first equation by a complex dielectric constant $\left[\epsilon + \mathrm{i}\sigma/\left(\omega\epsilon_0\right)\right] \to \epsilon$. Furthermore, we define $k = k_0\sqrt{\mu_\mathrm{r}\epsilon_\mathrm{r}}$, where $k_0 = \omega/c$ and $n = \sqrt{\mu_\mathrm{r}\epsilon_\mathrm{r}}$ is the index of refraction.

2.2 Angular spectrum representation

Let's suppose that we know a scalar field $f(x,y,0)$, which is a solution of a wave equation, at position $z = 0$, a natural question would be: how can we compute the field $f(x,y,z)$ at position z?

Using the Fourier transformed fields $\hat{f}\left(k_x,k_y\right)$, we start by decomposing the

initial field $f(x, y, 0)$ in a plane wave basis

$$f(x, y, 0) = (2\pi)^{-2} \int_{-\infty}^{\infty} \mathrm{e}^{\mathrm{i}(k_x x + k_y y)} \hat{f}\,(k_x, k_y)\,\mathrm{d}k_x \mathrm{d}k_y \tag{2.2.1}$$

When moving away from $z = 0$, we can make the general ansatz

$$f(x, y, z) = (2\pi)^{-3} \int_{-\infty}^{\infty} \mathrm{e}^{\mathrm{i}(k_x x + k_y y + k_z z)} \hat{f}\,(k_x, k_y, k_z)\,\mathrm{d}k_x \mathrm{d}k_y \mathrm{d}k_z. \tag{2.2.2}$$

However, wave equations like the ones seen in the previous sections impose constraints, so one degree of freedom is subtracted. We can thus express k_z for instance, in terms of the others

$$f(x, y, z) = (2\pi)^{-2} \int_{-\infty}^{\infty} \exp\left\{i\left[k_x x + k_y y + k_z\left(k_x, k_y\right) z\right]\right\} \hat{f}\,(k_x, k_y)\,\mathrm{d}k_x \mathrm{d}k_y \tag{2.2.3}$$

where we have explicitly indicated the dependence of $k_z = k_z\,(k_x, k_y)$. From this expression one observes that for $z > 0$ each plane wave acquires an additional phase

$$\mathrm{e}^{\mathrm{i}k_z z} \hat{f}\,(k_x, k_y)\,. \tag{2.2.4}$$

This factor is called the propagator in reciprocal space. On the other hand, if we consider the dispersion relation

$$\omega(k) = v|\mathbf{k}| = v\sqrt{k_x^2 + k_y^2 + k_z^2}, \qquad |\mathbf{k}| \equiv k \tag{2.2.5}$$

the k_z component has to be computed from

$$k_z = \pm\sqrt{k^2 - k_x^2 - k_y^2}. \tag{2.2.6}$$

The positive or negative sign has to be chosen for waves propagating in the positive or negative z direction. We can now distinguish two cases. For $k_x^2 + k_y^2 \leq k^2$ the z-component of the wavevector $k_z = \pm\sqrt{k^2 - k_x^2 - k_y^2}$ is a real number, corresponding to a normal wave propagation. However, for $k_x^2 + k_y^2 \geq k^2$ we get

$$k_z = \pm\sqrt{k^2 - k_x^2 - k_y^2} = \pm\mathrm{i}\sqrt{k_x^2 + k_y^2 - k^2} \equiv \pm\mathrm{i}\kappa, \tag{2.2.7}$$

which corresponds to evanescent waves. Thus, evanescent waves grow or decay exponentially when moving away from z. To be physically meaningful, we only keep the decaying waves, this is $\mathrm{e}^{-\kappa z}$ for $z > 0$ and $\mathrm{e}^{\kappa z}$ for $z < 0$. If we introduce these notions in Eq. 2.2.3 it is possible to express the fields at larger z values in the form

$$\begin{aligned} f(x,y,z) =& (2\pi)^{-2} \int_{k^2 > k_x^2 + k_y^2} \mathrm{e}^{\mathrm{i}\left(k_x x + k_y y + \sqrt{k^2 - k_x^2 - k_y^2} z\right)} \hat{f}\left(k_x, k_y\right) dk_x dk_y \\ &+ (2\pi)^{-2} \int_{k^2 < k_x^2 + k_y^2} \mathrm{e}^{\mathrm{i}(k_x x + k_y y) - \sqrt{k_x^2 + k_y^2 - k^2} z} \hat{f}\left(k_x, k_y\right) \mathrm{d}k_x \mathrm{d}k_y \end{aligned} \tag{2.2.8}$$

The same can be applied to a vector entity such as the electric field. Suppose we know the electric field distribution $\mathbf{E}_0(x, y)$ at a given plane $z = 0$, so it is also easy to find its Fourier decomposition $\hat{\mathbf{E}}_0\left(k_x, k_y\right)$. If we want to know the field for $z > 0$ we obtain, in accordance with the derivation of Eq. 2.2.8, the angular spectrum representation

$$\begin{aligned} \mathbf{E}(x,y,z) =& \int_{k^2 > k_x^2 + k_y^2} \mathrm{e}^{\mathrm{i}\left(k_x x + k_y y + \sqrt{k^2 - k_x^2 - k_y^2} z\right)} \ \hat{\mathbf{E}}_0\left(k_x, k_y\right) \mathrm{d}k_x \mathrm{d}k_y \\ &+ \int_{k^2 < k_x^2 + k_y^2} \mathrm{e}^{\mathrm{i}(k_x x + k_y y) - \sqrt{k_x^2 + k_y^2 - k^2} z} \ \hat{\mathbf{E}}_0\left(k_x, k_y\right) \mathrm{d}k_x \mathrm{d}k_y \end{aligned} \tag{2.2.9}$$

Hence, we find that the angular spectrum is indeed a superposition of plane waves and evanescent waves, or in other words, the contribution to the electric field can be separated into real and virtual photons. From this equation one observes that in order to compute fields away from a given plane we must first decompose $\mathbf{E}(x, y, 0)$ into its Fourier components, and then each Fourier component simply acquires a phase or decays exponentially when moving away from $z = 0$.

For this investigation only propagating waves will be used, so we can continue developing a more suitable expression to represent far-fields in the angular spectrum representation, i.e. in the evaluation of the field at a point $\mathbf{r} = \mathbf{r}_\infty$ at an infinite distance from the object plane. To calculate the far-field $\mathbf{E}_\infty$ we require the limit $kr \to \infty$,

$$\mathbf{E}_\infty\left(\mathbf{n}_x, \mathbf{n}_y\right) = \lim_{kr \to \infty} \int_{\left(k_x^2 + k_y^2\right) \leq k^2} \hat{\mathbf{E}}\left(k_x, k_y; 0\right) \mathrm{e}^{\mathrm{i}k\mathbf{r}\left[\frac{k_x}{k}\mathbf{n}_x + \frac{k_y}{k}\mathbf{n}_y \pm \frac{k_z}{k}\mathbf{n}_z\right]} \mathrm{d}k_x \ \mathrm{d}k_y \tag{2.2.10}$$

where $\mathbf{n}_i$ is an unit vector in the i^{th} direction, and $\mathbf{n}_z = \mathbf{n}_z(\mathbf{n}_x, \mathbf{n}_y)$. Fortunately, the stationary phase approximation [26] provides a recipe for dealing with such integrals, which allows us to write

$$\mathbf{E}_\infty(\mathbf{n}_x, \mathbf{n}_y) = -2\pi \mathrm{i} k_z \hat{\mathbf{E}}(k_x, k_y; 0) \frac{\mathrm{e}^{\mathrm{i}kr}}{r}. \tag{2.2.11}$$

This equation tells us that the far-fields are entirely defined by the Fourier spectrum of the fields $\hat{\mathbf{E}}(k_x, k_y; 0)$ which implies that only one plane wave with the wavevector $k = (k_x, k_y, k_z)$ of the angular spectrum at $z = 0$ contributes to the far-field at a point located in the direction of the unit vector $\mathbf{n} = (\mathbf{n}_x, \mathbf{n}_y, \mathbf{n}_z)$. The effect of all other plane waves is cancelled out by destructive interference. This result allows us to treat the field in the far-zone as a collection of rays with each ray being characterized by a particular plane wave, similar to what we know from geometrical optics. After clearing $\hat{\mathbf{E}}$ and replacing it into the angular spectrum representation Eq. 2.2.9, we find

$$\mathbf{E}(x, y, z) = \frac{\mathrm{i}r\mathrm{e}^{-\mathrm{i}kr}}{2\pi} \int_{\left(k_x^2 + k_y^2\right) \leq k^2} \mathbf{E}_\infty\left(\frac{k_x}{k}, \frac{k_y}{k}\right) \mathrm{e}^{\mathrm{i}[k_x x + k_y y \pm k_z z]} \frac{1}{k_z} \, \mathrm{d}k_x \, \mathrm{d}k_y, \tag{2.2.12}$$

which is a useful way to express far-fields in the angular spectrum representation.

2.3 Light-Matter

We are usually interested in studying a system from an energy perspective. This is the framework that gives us the Hamiltonian formalism. It is well known that for a free charge q with mass m in an external electromagnetic field we have [27]

$$H_{\text{particle}} = \frac{1}{2m}(\boldsymbol{p} - q\mathbf{A})^2 + q\phi. \tag{2.3.1}$$

where $\boldsymbol{p} = m\boldsymbol{v} + q\mathbf{A}$ is the canonical momentum, which is the sum of mechanical momentum $m\boldsymbol{v}$ and field momentum $q\mathbf{A}$. However, this Hamiltonian does not account for the total energy "charge plus field", since neither the energy of the electromagnetic field nor the interaction between charges (as in the case of atoms or molecules) are included. As usual in the study of light-matter interaction, the total

Hamiltonian can be separated into one for the field, one for the particle, and one for the interaction between them,

$$H_{\text{tot}} = H_{\text{particle}} + H_{\text{rad}} + H_{\text{int}}.$$

Using the electromagnetic potentials $\mathbf{A}$ and ϕ, defined in the Eqs. 2.1.16 and 2.1.17, together with its gauge freedom, it is possible to derive [28]

$$H_{\text{int}} = -\frac{q}{m}\mathbf{A}\left(\mathbf{r},t\right)\cdot\boldsymbol{p} + \frac{q^2}{2m}\mathbf{A}\left(\mathbf{r},t\right)\cdot\mathbf{A}\left(\mathbf{r},t\right) + q\phi\left(\mathbf{r},t\right)]. \tag{2.3.2}$$

However, this Hamiltonian is not unique, since it is not gauge invariant. To remove the ambiguity it is necessary to express H_{int} in terms of the physical fields $\mathbf{E}$ and $\mathbf{B}$. For this it is necessary to write $\mathbf{A} = \mathbf{A}(\mathbf{E},\mathbf{B})$ and $\phi = \phi(\mathbf{E},\mathbf{B})$. Those expansions have been determined by [29],

$$\phi(\mathbf{r}) = \phi(0) - \sum_{i=0}^{\infty}\frac{\mathbf{r}[\mathbf{r}\cdot\nabla]^i}{(i+1)!}\cdot\mathbf{E}(0), \quad \mathbf{A}(\mathbf{r}) = \sum_{i=0}^{\infty}\frac{[\mathbf{r}\cdot\nabla]^i}{(i+2)i!}\mathbf{B}(0)\times\mathbf{r}.$$

Plugging them into 2.3.2 we get the so-called Hamiltonian of multipole interaction,

$$H_{\text{int}} \ = q_{\text{tot}}\,\phi(0,t) - \mathbf{p}\cdot\mathbf{E}(0,t) - \mathbf{m}\cdot\mathbf{B}(0,t) - [\overleftrightarrow{\mathbf{Q}}\,\nabla]\cdot\mathbf{E}(0,t) - \cdots \tag{2.3.3}$$

where q_{tot} is the total charge of the system, $\mathbf{p}$ and $\mathbf{m}$ are their electric and magnetic dipole moment, and $\overleftrightarrow{\mathbf{Q}}$ the total electric quadrupole moment. If the system of charges is neutral, the first term is null. Furthermore, if we focus on the electric dipole transition that interchange the $S \to P$ (see Chapter 5) orbitals, we can neglect the first-order magnetic contribution and focus only on the $-\mathbf{p}\cdot\mathbf{E}$ term, which tells us that we can treat the most elementary radiative neutral object as an electric dipole, at least to first order.

2.4 Dyadic Green Functions

Suppose there is an inhomogeneous differential equation that determines the response of a system, represented by the vector function $\mathbf{R}$, given a source function

S. This equation could be written as

$$\mathcal{L}\mathbf{R}(\mathbf{r}) = \mathbf{S}(\mathbf{r}) \tag{2.4.1}$$

where $\mathcal{L}$ is a linear differential operator. A well-known theorem for linear differential equations states that the general solution is equal to the sum of the complete homogeneous solution ($\mathbf{S} = 0$) and a particular inhomogeneous solution. If we assume that we know the homogeneous solution ($\mathbf{R}_0$), thus we need to solve for an arbitrary particular solution only. A convenient option is to first find a solution with a point source $\delta(\mathbf{r})$, from which an important concept in field theory is derived: the Green function, the fields due to a point source. But these functions can be separated into at least two families, depending on whether the vector direction of the source matches the direction of the generated field. For example, a source current in x-axis gives rise to a potential vector with just an x-component. Instead, a source current in x-axis leads to an electric and magnetic field with x-, y-, and z-components. Thus, in the case of the electric and magnetic fields we need a Green function that relates all components of the source to all components of the fields, i.e. the Green function must be a tensor. This type of Green function is called a **dyadic Green function**, and is a way to write three differential equations with vectors as source and response functions in a compact form,

$$\mathcal{L}\overset{\leftrightarrow}{\mathbf{G}}(\mathbf{r}, \mathbf{r}') = \overset{\leftrightarrow}{\mathbf{I}}\,\delta^3(\mathbf{r} - \mathbf{r}') \tag{2.4.2}$$

where the operator $\mathcal{L}$ acts on each column of $\overset{\leftrightarrow}{\mathbf{G}}$ separately and $\overset{\leftrightarrow}{\mathbf{I}}$ is the unit dyad. In general, the vector field $\overset{\leftrightarrow}{\mathbf{G}} \cdot\mathbf{n}$, where $\mathbf{n}$ is a generic unit vector, depends on the location $\mathbf{r}'$ of the inhomogeneity $\delta^3(\mathbf{r} - \mathbf{r}')$, so the Green's tensor has as argument both the place of measurement $\mathbf{r}$ and the place of the source $\mathbf{r}'$. Multiplying the Eq. 2.4.2 by $\mathbf{S}(\mathbf{r}')$ and integrating in a volume containing the sources, we obtain

$$\int_V \mathcal{L}\overset{\leftrightarrow}{\mathbf{G}}(\mathbf{r}, \mathbf{r}')\,\mathbf{S}(\mathbf{r}')\,\mathrm{d}V' = \int_V \mathbf{S}(\mathbf{r}')\,\delta^3(\mathbf{r} - \mathbf{r}')\,\mathrm{d}V' = \mathbf{S}(\mathbf{r}) = \mathcal{L}\mathbf{R}(\mathbf{r}). \tag{2.4.3}$$

If on the right-hand side the operator $\mathcal{L}$ is taken out of the integral, the solution of Eq. 2.4.1 can be expressed as

$$\mathbf{R}(\mathbf{r}) = \int_V \overset{\leftrightarrow}{\mathbf{G}}(\mathbf{r}, \mathbf{r}') \, \mathbf{S}(\mathbf{r}') \, \mathrm{d}V' \tag{2.4.4}$$

This tells us that the way the function $\mathbf{R}$ behaves due to the presence of S is given by the Green function. For this reason, it is said that $\overset{\leftrightarrow}{\mathbf{G}}$ connects both phenomena.

With this in mind, let us derive the dyadic Green's function for the electric field. For this we can consider an arbitrary reference system whose dielectric properties are represented by a spatially inhomogeneous dielectric constant $\epsilon(\mathbf{r}) = \epsilon_0 \epsilon_\mathrm{r}(\mathbf{r})$. Commonly, non-magnetic and isotropic materials are used as reference, for which $\mu_\mathrm{r} = 1$, but we will keep it in the notation to arrive at a more general case with $\mu(\mathbf{r}) = \mu_0 \mu_\mathrm{r}(\mathbf{r})$. In the previous section we used Maxwell's equations 2.1.22 and 2.1.24 together with the constitutive relations to derive a wave equation for the electric field, Eq. 2.1.28, which can be rewritten as

$$\left[\nabla \times \nabla \times \, - \frac{\omega^2}{c^2} \mu_\mathrm{r} \epsilon_\mathrm{r} \right] \mathbf{E}(\mathbf{r}) = \mathrm{i}\omega \mu_0 \mu \mathbf{j}_s(\mathbf{r}). \tag{2.4.5}$$

To know the solution of this operator whatever the direction of a point source, we can look for its dyadic Green's function $\overset{\leftrightarrow}{\mathbf{G}}$. For this we need to solve

$$\left[\nabla \times \nabla \times \, - \frac{\omega^2}{c^2} \mu_\mathrm{r} \epsilon_\mathrm{r}(\mathbf{r}) \right] \overset{\leftrightarrow}{\mathbf{G}}(\mathbf{r}, \mathbf{r}') = \overset{\leftrightarrow}{\mathbf{I}} \delta^3(\mathbf{r} - \mathbf{r}'), \tag{2.4.6}$$

so, by direct comparison with Eq. 2.4.4, the electric field can be represented as

$$\mathbf{E}(\mathbf{r}) = \mathbf{E}_0(\mathbf{r}) + \frac{\mathrm{i}\omega}{\epsilon_0 c^2} \mu \int_V \overset{\leftrightarrow}{\mathbf{G}}(\mathbf{r}, \mathbf{r}') \, \mathbf{j}_\mathrm{s}(\mathbf{r}') \, \mathrm{d}V' \tag{2.4.7}$$

where the volume element $\mathrm{d}V'$ indicates an integration over the region of the emitting objects, of position $\mathbf{r}'$. The $\mathbf{E}_0$ term denotes the homogeneous solution with $\mathbf{j}_\mathrm{s} = 0$. The current density of an electric dipole with moment $\mathbf{p}_0$ located at $\mathbf{r} = \mathbf{r}'$ is

$$\mathbf{j}_\mathrm{s}(\mathbf{r}) = -\mathrm{i}\omega \mathbf{p}_0 \delta^3(\mathbf{r} - \mathbf{r}') \tag{2.4.8}$$

If the external excitations are null and the field is produced exclusively by the dipoles, inserting this current into Eq. 2.4.7 the electromagnetic fields can be expressed in terms of $\overleftrightarrow{\mathbf{G}}(\mathbf{r},\mathbf{r}')$ as

$$\mathbf{E}(\mathbf{r}) = \frac{\omega^2}{\epsilon_0 c^2}\mu\, \overleftrightarrow{\mathbf{G}}(\mathbf{r},\mathbf{r}')\,\mathbf{p}_0 \tag{2.4.9}$$

Thus, the field produced by an arbitrarily oriented dipole located at $\mathbf{r}_0$ is given by the Green's function $\overleftrightarrow{\mathbf{G}}(\mathbf{r},\mathbf{r}')$, which can be separated into two terms

$$\overleftrightarrow{\mathbf{G}}(\mathbf{r},\mathbf{r}') = \overleftrightarrow{\mathbf{G}}_0(\mathbf{r},\mathbf{r}') + \overleftrightarrow{\mathbf{G}}_{\mathrm{S}}(\mathbf{r},\mathbf{r}'), \tag{2.4.10}$$

where the primary part $\overleftrightarrow{\mathbf{G}}_0$ determines the direct dipole field and can be expressed as

$$\overleftrightarrow{\mathbf{G}}_0(\mathbf{r},\mathbf{r}') = \left[\overleftrightarrow{\mathbf{I}} + \frac{1}{k^2}\nabla\nabla\right] G_0(\mathbf{r},\mathbf{r}'). \tag{2.4.11}$$

in which the scalar Green's function function $G_0(\mathbf{r},\mathbf{r}')$ is the solution for the Helmholtz operator

$$\left[\nabla^2 + k^2\right] G_0(\mathbf{r},\mathbf{r}') = -\delta^3(\mathbf{r}-\mathbf{r}') \tag{2.4.12}$$

with a single point source $\delta^3(\mathbf{r}-\mathbf{r}')$. In free space, the only physical solution of this equation is [27]

$$G_0(\mathbf{r},\mathbf{r}') = \frac{\mathrm{e}^{\pm \mathrm{i}k|\mathbf{r}-\mathbf{r}'|}}{4\pi\,|\mathbf{r}-\mathbf{r}'|}, \tag{2.4.13}$$

which allows us to calculate the free space Green's function

$$\overleftrightarrow{\mathbf{G}}_0(\mathbf{r},\mathbf{r}') = \frac{\exp(\mathrm{i}kR)}{4\pi R}\left[\left(1+\frac{\mathrm{i}kR-1}{k^2R^2}\right)\overleftrightarrow{\mathbf{I}} + \frac{3-3\mathrm{i}kR-k^2R^2}{k^2R^2}\frac{\mathbf{RR}}{R^2}\right], \tag{2.4.14}$$

which fulfills the condition $\overleftrightarrow{\mathbf{G}}_0(\mathbf{r},\mathbf{r}',\omega) \to 0$ as $|\mathbf{r}-\mathbf{r}'| \to \infty$. One can separate the contributions to the field in terms of the distance between the emitter and the receiver,

$$\overleftrightarrow{\mathbf{G}}_0 = \overleftrightarrow{\mathbf{G}}_{\mathrm{NF}} + \overleftrightarrow{\mathbf{G}}_{\mathrm{IF}} + \overleftrightarrow{\mathbf{G}}_{\mathrm{FF}} \tag{2.4.15}$$

where the near-field (G_{NF}), intermediate-field (G_{IF}), and far-field (G_{FF}) Green func-

tions are given by

$$\overleftrightarrow{\mathbf{G}}_{\mathrm{NF}}=\frac{\exp(\mathrm{i}kR)}{4\pi R}\frac{1}{k^2R^2}\left[-\overleftrightarrow{\mathbf{I}}+3\mathbf{RR}/R^2\right], \tag{2.4.16}$$

$$\overleftrightarrow{\mathbf{G}}_{\mathrm{IF}}=\frac{\exp(\mathrm{i}kR)}{4\pi R}\frac{\mathrm{i}}{kR}\left[\overleftrightarrow{\mathbf{I}}-3\mathbf{RR}/R^2\right], \tag{2.4.17}$$

$$\overleftrightarrow{\mathbf{G}}_{\mathrm{FF}}=\frac{\exp(\mathrm{i}kR)}{4\pi R}\left[\overleftrightarrow{\mathbf{I}}-\mathbf{RR}/R^2\right]. \tag{2.4.18}$$

As expected, the radiative content of the dipole at long distances is given by (G_{FF}), while the other terms ($G_{\mathrm{NF}}, G_{\mathrm{IF}}$) accounts for short-range contributions (or evanescent field).

The secondary electromagnetic field, i.e. the field that is reflected from or transmitted through inhomogeneities in the environment, is given by the scattering part of the Green's function $\overleftrightarrow{\mathbf{G}}_{\mathrm{S}}$. This description [28] indicates that if we want to account for the field passing through an aplanatic lens, we must look for a scattering Green's function.

2.5 Emission Rate

In the middle of the 20th century, the mechanism through which atoms emitted radiation was unknown, so it was considered an intrinsic characteristic without further development. A study of the emission of a nuclear magnetic moment coupled to a resonant electronic device published by Purcell [30] showed that it is possible to modify the decay rate by modifying the environmental conditions. Since then, alterations in the emission rate due to planar interfaces, cavities, photonic crystals and optical antennas have been verified [31–35].

The first approximation of the rate of decay comes from the Fermi's golden rule, usually written as

$$\Gamma=\frac{2\pi}{\hbar^2}\sum_f\left|\left\langle f\left|\hat{H}_{\mathrm{I}}\right|i\right\rangle\right|^2\delta\left(\omega_i-\omega_f\right) \tag{2.5.1}$$

where $\hat{H}_{\mathrm{I}}=-\hat{\mathbf{d}}\cdot\hat{\mathbf{E}}$ is the Hamiltonian of interaction between the atom (treated as a dipole) and the external field. In what follows, only the most relevant facts will be given to arrive at an expression for the emission rate in terms of the dyadic Green's

function.

First, we need to define the initial and final state of the combined system "field plus atom" as

$$|i\rangle = |e, \{0\}\rangle = |e\rangle|\{0\}\rangle \tag{2.5.2}$$

$$|f\rangle = \left|g, \left\{1(\mathbf{r}, \omega, \hat{\mathbf{k}})\right\}\right\rangle = |g\rangle \left|\left\{1(\mathbf{r}, \omega, \hat{\mathbf{k}})\right\}\right\rangle \tag{2.5.3}$$

respectively. Here, $|\{0\}\rangle$ denotes the zero-photon state, and $\left|\left\{1(\mathbf{r}, \omega, \hat{\mathbf{k}})\right\}\right\rangle$ designates the onephoton state associated with mode and frequency $\omega = (E_{\mathrm{e}} - E_{\mathrm{g}})/\hbar$. In a Green-tensor notation, we can express the interaction field as (see Eq. 3.0.12)

$$\begin{aligned} H_{AF} &= -\,\hat{\mathbf{d}} \cdot \hat{\mathbf{E}}\,(r_A) && (2.5.4)\\ &= \sum_{\lambda} \int \mathrm{d}^3 r \int \mathrm{d}\omega \mathbf{d}^{\dagger} \cdot \overset{\leftrightarrow}{\mathbf{G}}\,(\mathbf{r}_A, \mathbf{r}, \omega) \cdot \hat{\mathbf{f}}(\mathbf{r}, \omega)\ \hat{\sigma}_+ \\ &\quad + \hat{\mathbf{f}}^{\dagger}(\mathbf{r}, \omega) \cdot \overset{\leftrightarrow}{\mathbf{G}}{}^{\dagger}\,(\mathbf{r}_A, \mathbf{r}, \omega) \cdot \mathbf{d}\ \hat{\sigma}_-, && (2.5.5) \end{aligned}$$

where $\lambda = e, m$ accounts for the elementary electric and magnetic excitations of the system, its possible to write the transition $|i\rangle \longrightarrow |f\rangle$ as

$$\left\langle g \left| \left\langle \{0\} \left| \left(-\hat{\mathbf{d}} \cdot \hat{\mathbf{E}}\,(\mathbf{r}_A)\right) \right| e \right\rangle \right| 1_{\lambda}(\mathbf{r}, \omega, \hat{\mathbf{k}}) \right\rangle = \mathbf{d}_{ge} \cdot \overset{\leftrightarrow}{\mathbf{G}}\,(\mathbf{r}_A, \mathbf{r}, \omega) \cdot \hat{\mathbf{k}} \tag{2.5.6}$$

where we have defined the electric dipole operator as $\hat{\mathbf{d}} = \mathbf{d}_{eg}|e\rangle\langle g| + \mathbf{d}_{ge}|g\rangle\langle e|$. Now, using the fluctuation-dissipation relation for a non-magnetic medium $\mu = \mu_0$ [36],

$$\sum_{\lambda} \int \mathrm{d}^3 r\ \overset{\leftrightarrow}{\mathbf{G}}_{\lambda}\,(\mathbf{r}_1, \mathbf{r}, \omega) \cdot \overset{\leftrightarrow}{\mathbf{G}}{}^{\dagger}_{\lambda}\,(\mathbf{r}_2, \mathbf{r}, \omega) = \frac{\hbar \mu_0 \omega^2}{\pi}\, \mathrm{Im}\ \overset{\leftrightarrow}{\mathbf{G}}\,(\mathbf{r}_1, \mathbf{r}_2, \omega)\,, \tag{2.5.7}$$

we can write the Fermi's golden rule as

$$\Gamma(\mathbf{r}_A, \mathbf{r}_A, \omega) = \frac{2\mu_0 \omega^2}{\hbar} \mathbf{d}_{ge} \cdot \mathrm{Im}\ \overset{\leftrightarrow}{\mathbf{G}}\,(\mathbf{r}_A, \mathbf{r}_A, \omega) \cdot \mathbf{d}_{eg}, \tag{2.5.8}$$

where $\mathbf{d}_{ge}$ denotes the transition dipole matrix element. A more detailed explanation can be found in the references [28, 36].

The formalism of the dyadic Green functions allows us to discriminate the nature of the emission according to the conditions of the environment in which the emitting object is found. As Eq. 2.4.10, the Green's tensor can be separated into one for the free-space $\overleftrightarrow{\mathbf{G}}_0$ and one for the perturbations of the neighborhood $\overleftrightarrow{\mathbf{G}}_\mathrm{S}$, which can be of a purely geometric character.

If we make a Taylor approximation of $\overleftrightarrow{\mathbf{G}}_0$, given by Eq. 2.4.14, in the neighborhood of $\mathbf{r} = \mathbf{r}_A$, we will obtain

$$\mathrm{Im}\ \overleftrightarrow{\mathbf{G}}_0\ (\mathbf{r}_A, \mathbf{r}_A, \omega) = \frac{\omega}{6\pi c}\ \overleftrightarrow{\mathbf{I}}, \tag{2.5.9}$$

so if we introduce it into Eq. 2.5.8 we arrive to the well-known spontaneous emission rate for an atom in free-space

$$\gamma_0 = \frac{\omega_0^3 \mathbf{d}_{ge}^2}{3\pi\varepsilon_0 \hbar c^3} \tag{2.5.10}$$

The inhomogeneities of the environment lead to modifications in the total emission rate Γ_tot [30]. If the position $\mathbf{r}_A$ and the transition frequency of the atom ω_0 are fixed, and only the position of the source is left as a variable,

$$\Gamma_\mathrm{tot}(\mathbf{r}) = \gamma_0 + \Gamma'(\mathbf{r}), \tag{2.5.11}$$

being $\Gamma'(\mathbf{r})$ the position dependent modification of the emission, given by

$$\Gamma'(\mathbf{r}) = \frac{2\mu_0\omega_0^2}{\hbar}|\mathbf{d}|^2 \mathbf{n}_d \cdot \mathrm{Im}\ \overleftrightarrow{\mathbf{G}}_\mathrm{S}\ (\mathbf{r}_A, \mathbf{r}, \omega_0) \cdot \mathbf{n}_d, \tag{2.5.12}$$

which depends on the orientation of the dipole $\mathbf{n}_d$ and the dipole moment $|\mathbf{d}|^2$ specific for each atomic transition of a particular atom [37]. Naturally, this opens up a palette of possibilities. In cases where the atom is driven by circularly polarized light, i.e. photons with σ^+ or σ^- polarization, the light transfers its angular momentum to the atom. After a long time compared with γ_0^{-1}, the atomic population is transferred to the state with the highest angular momentum, limiting the accessible states and transforming the atom into an effective two-level system. The case of a cyclic transitions $\langle J, F, m_F || J', F', m_{F'} \rangle$ with circularly polarized light, the transition carries with it a degeneracy factor of $(2J+1)/(2J'+1)$, so the dipole moment

will be given by

$$\left|\mathbf{d}_{m_F \to m_{F'}}\right|^2 = \frac{2J+1}{2J'+1} \left|\langle J \| er \| J' \rangle\right|^2 \tag{2.5.13}$$

Finally, it is important to distinguish between transition rates, decay rates and scattering rates. The transition rates depend on the respective dipole matrix elements and the imaginary part of Green's tensor taken at the atomic transitions frequencies. For simplicity, we will call it just $\Gamma_{\text{trans.}}$. The total decay rate of an excited state is obtained by summing the transition rates to all lower lying states, so you would have to evaluate Eq. 2.5.8 for each of them with its characteristic $|\mathbf{d}|$ and then add them together. If there are n possible transitions involved, then de decay rate is given by $\Gamma_{\text{decay}} = \sum_n \Gamma_{\text{trans.},\, n}$. The scattering rate takes into account the probability that the atom is excited. Let's call that probability ρ_{ee}. Then $\Gamma_{\text{scatt.}} = \rho_{ee}\Gamma_{\text{decay}}$. For a two-level atom there is only one transition allowed, so we can refer of transition rate and decay rate interchangeably. For example, Eq. 2.5.11 refers only to a cyclic transition for a two-level atom, so $\Gamma_{\text{trans.}} = \Gamma_{\text{tot}}$.

Chapter 3

Master Equation

While the evolution of the state vector in a closed quantum system is deterministic, open quantum systems are stochastic in nature. The environment induces stochastic transitions between energy levels, and to introduce uncertainty in the phase difference between states of the system. The state of an open quantum system is described by a density matrix $\hat{\rho}_{\text{tot}}$ which describes a probability distribution of quantum states. In a matrix representation, $\hat{\rho}_{\text{tot}} = \sum_n p_n \left|\psi_n\right\rangle \left\langle\psi_n\right|$, where p_n is the classical probability that the system is in the quantum state $\left|\psi_n\right\rangle$. To derive the equation of motion for an open quantum system we have to expand the scope of the system to include the environment and convert it into a closed quantum system, whose evolution is given, in Schrödinger picture, by

$$\frac{\partial \hat{\rho}_{\text{tot}}}{\partial t} = -\frac{\mathrm{i}}{\hbar}\left[H, \hat{\rho}_{\text{tot}}\right] \tag{3.0.1}$$

When solved for all times, it provides a full characterization of the states of both the system and the reservoir. Here we consider a generic system S consisting of a subsystem $S\text{b}$ coupled to a large reservoir R by some interaction I. That decomposition of the system will be represented by their respective Hamiltonians

$$S\text{b} \quad \longrightarrow \quad H_A, \tag{3.0.2}$$

$$R \quad \longrightarrow \quad H_F, \tag{3.0.3}$$

$$I \quad \longrightarrow \quad H_{AF}, \tag{3.0.4}$$

where H_A is the atom Hamiltonian, H_F is the field Hamiltonian and H_{AF} is the interaction Hamiltonian. If we add each part of the whole generic system, we will have

$$H_S = H_A + H_F + H_{AF} \equiv H_0 + H_{AF}. \tag{3.0.5}$$

Since we are only interested in the behavior of the subsystem, we can perform a partial trace over the environmental degrees of freedom in Eq. 3.0.1, and thereby obtain the dynamics of $\hat{\rho}_A = \mathrm{Tr}_F\left[\hat{\rho}_{\mathrm{tot}}\right]$ which is called the master equation of the original system density matrix [38],

$$\dot{\hat{\rho}}_A = -\mathrm{i}[H, \hat{\rho}_A] + \sum_m \left(L_m \hat{\rho}_A L_m^\dagger - \frac{1}{2}\left\{ L_m^\dagger L_m, \hat{\rho}_A \right\} \right) \tag{3.0.6}$$

where the L_m are collapse operators through which the environment couples to the system in H_{AF}, and which will give us the dissipation rate of the open system. This equation provides us, in the Schördinger picture, a partial and simplified description that allows us to achieve the limited goal to determine the evolution of the subsystem only. Assuming that the system and reservoir are brought into contact at time $t = t_0$, they initially do not exhibit any correlations and thus the initial state of the system is described by the factorized density operator

$$\hat{\rho}_{\mathrm{tot}}\left(t_0\right) = \hat{\rho}_A\left(t_0\right) \otimes \hat{\rho}_R\left(H_F\right), \tag{3.0.7}$$

where $\hat{\rho}_R\left(H_F\right) = |\{0\}\rangle\langle\{0\}|$ is the initial state of the reservoir. This requirement will continue to be required when there is a non-zero interaction, which is called the Born approximation. To do the calculations, we have to specify the way in which both parts interact and by which the separability condition will be obsolete. But first, it is constructive to note that the atomic and field Hamiltonians are given by [36],

$$H_A = \sum_{i=1}^{N} \hbar\omega_0 \hat{\sigma}_+^{(i)} \hat{\sigma}_-^{(i)} \tag{3.0.8}$$

$$H_F = \int \mathrm{d}^3 r \int \mathrm{d}\omega \hbar\omega \hat{\mathbf{f}}^\dagger(\mathbf{r}, \omega) \hat{\mathbf{f}}(\mathbf{r}, \omega), \tag{3.0.9}$$

Where ω_0 is the angular frequency associated with the transition between the excited state and the ground-state of a two-level atom, and where $\hat{\mathbf{f}}(\mathbf{r},\omega)$ and $\hat{\mathbf{f}}^{\dagger}(\mathbf{r},\omega)$ are bosonic operators which obey the canonical commutation relations

$$\left[\hat{\mathbf{f}}(\mathbf{r},\omega),\hat{\mathbf{f}}\left(\mathbf{r}',\omega'\right)\right]=\left[\hat{\mathbf{f}}^{\dagger}(\mathbf{r},\omega),\hat{\mathbf{f}}^{\dagger}\left(\mathbf{r}',\omega'\right)\right]=0 \tag{3.0.10}$$

$$\left[\hat{\mathbf{f}}(\mathbf{r},\omega),\hat{\mathbf{f}}^{\dagger}\left(\mathbf{r}',\omega'\right)\right]=\delta\left(\mathbf{r}-\mathbf{r}'\right)\delta\left(\omega-\omega'\right). \tag{3.0.11}$$

The interaction between the two-level atom and the external field is given by

$$\begin{aligned}H_{AF}=&\sum_{i=1}^{N}\int \mathrm{d}^3r\int \mathrm{d}\omega\mathbf{d}^{\dagger}\cdot\overleftrightarrow{\mathbf{G}}_e\left(\mathbf{r}_i,\mathbf{r},\omega_0\right)\cdot\hat{\mathbf{f}}(\mathbf{r},\omega)\;\hat{\sigma}_{+}^{(i)}\\&+\hat{\mathbf{f}}^{\dagger}(\mathbf{r},\omega)\cdot\overleftrightarrow{\mathbf{G}}_e^{\dagger}\left(\mathbf{r}_i,\mathbf{r},\omega\right)\cdot\mathbf{d}\;\hat{\sigma}_{-}^{(i)}.\end{aligned} \tag{3.0.12}$$

where, for simplicity and without ambiguity, we will change to the notation $\mathbf{d}_{eg}\rightarrow\mathbf{d}$ and $\mathbf{d}_{ge}\rightarrow\mathbf{d}^{\dagger}$. Also, $\overleftrightarrow{\mathbf{G}}_e$ is defined by [39]

$$\overleftrightarrow{\mathbf{G}}_e\left(\mathbf{r}_i,\mathbf{r},\omega\right)=\mathrm{i}\frac{\omega^2}{\epsilon_0c^2}\sqrt{\frac{\hbar\epsilon_0}{\pi}\operatorname{Im}\epsilon_{\mathrm{r}}\left(\mathbf{r},\omega\right)}\;\overleftrightarrow{\mathbf{G}}\left(\mathbf{r}_i,\mathbf{r},\omega\right) \tag{3.0.13}$$

It is important to note that throughout this chapter we will assume a non-magnetic medium ($\mu_{\mathrm{r}}=1$), so Eq. 3.0.12 holds. Although these Hamiltonians are general for generic atom-field interactions, in the chapter 5 it will be reduced to the specific case in which H_F accounts for the field produced by the atoms, H_{AF} accounts for the effect of photons emitted by atoms at one end of the lens on atoms at the other end, and so the energy of the atoms H_A will be modified by the presence of an external drive with detuning $\delta_D=\omega_0-\omega_D$. For this reason of generality, it will not be imposed the monochromatic condition on H_{AF} throughout the derivation of an expression for $\dot{\hat{\rho}}_A$. For now, let us continue the general case.

In order to obtain this goal, we change the frame of reference to a rotating frame with respect to the total free Hamiltonian H_A+H_F. The interaction Hamiltonian

at time t can be rewritten then as

$$H_{AF}(t) = \sum_{i=1}^{N} \int \mathrm{d}^3 r \int \mathrm{d}\omega \mathbf{d}^\dagger \cdot \overleftrightarrow{\mathbf{G}}_e \left(\mathbf{r}_i, \mathbf{r}, \omega\right) \cdot \hat{\mathbf{f}}(\mathbf{r}, \omega) \left(\hat{\sigma}_+^{(i)} e^{-i\delta_- t}\right) + \hat{\mathbf{f}}^\dagger(\mathbf{r}, \omega) \cdot \overleftrightarrow{\mathbf{G}}_e^\dagger \left(\mathbf{r}_i, \mathbf{r}, \omega\right) \cdot \mathbf{d} \left(\hat{\sigma}_-^{(i)} e^{i\delta_- t}\right) \tag{3.0.14}$$

where $\delta_\pm = (\omega \pm \omega_0)$. We now consider the Born-Markov master equation for the atom density matrix evolution [40],

$$\frac{\mathrm{d}\rho_A}{\mathrm{d}t} = -\frac{1}{\hbar^2} \mathrm{Tr}_F \int_0^\infty \mathrm{d}\tau \left[H_{AF}(t), \left[H_{AF}(t-\tau), \rho_A \otimes |0\rangle\langle 0|\right]\right]. \tag{3.0.15}$$

Expanding the commutators, we can separate four terms

$$\begin{aligned} \frac{\mathrm{d}\rho_A}{\mathrm{d}t} = &\underbrace{-\frac{1}{\hbar^2} \mathrm{Tr}_F \int_0^\infty \mathrm{d}\tau H_{AF}(t) H_{AF}(t-\tau) \rho_A \otimes |0\rangle\langle 0|}_{\text{(I)}} \\ &\underbrace{-\frac{1}{\hbar^2} \mathrm{Tr}_F \int_0^\infty \mathrm{d}\tau \rho_A \otimes |0\rangle\langle 0| H_{AF}(t-\tau) H_{AF}(t)}_{\text{(II)}} \\ &\underbrace{+\frac{1}{\hbar^2} \mathrm{Tr}_F \int_0^\infty \mathrm{d}\tau H_{AF}(t) \rho_A \otimes |0\rangle\langle 0| H_{AF}(t-\tau)}_{\text{(III)}} \\ &\underbrace{+\frac{1}{\hbar^2} \mathrm{Tr}_F \int_0^\infty \mathrm{d}\tau H_{AF}(t-\tau) \rho_A \otimes |0\rangle\langle 0| H_{AF}(t)}_{\text{(IV)}}. \end{aligned} \tag{3.0.16}$$

Those terms are calculated in detail in the appendix 7.1. For clarity, it will suffice to indicate that by expanding the term (I) we will obtain

$$
\begin{aligned}
(\mathrm{I}) = -\frac{1}{\hbar^2}\,\mathrm{Tr}_F \int_0^\infty \mathrm{d}\tau \Bigg[\sum_{i=1}^{N} \int \mathrm{d}^3 r \int \mathrm{d}\omega \left(\hat{\sigma}_+^{(i)} e^{-i\delta_- t}\right) \mathbf{d}^\dagger \cdot \overleftrightarrow{\mathbf{G}}_e\left(\mathbf{r}_i, \mathbf{r}, \omega\right) \cdot \hat{\mathbf{f}}(\mathbf{r}, \omega) \\
+ \hat{\mathbf{f}}^\dagger(\mathbf{r}, \omega) \cdot \overleftrightarrow{\mathbf{G}}_e^\dagger\left(\mathbf{r}_i, \mathbf{r}, \omega\right) \cdot \mathbf{d} \left(\hat{\sigma}_-^{(i)} e^{i\delta_- t}\right) \Bigg] \times \qquad (3.0.17) \\
\Bigg[\sum_{j=1}^{N} \int \mathrm{d}^3 r' \int \mathrm{d}\omega \left(\hat{\sigma}_+^{(j)} e^{-i\delta_-(t-\tau)}\right) \mathbf{d}^\dagger \cdot \overleftrightarrow{\mathbf{G}}_e\left(\mathbf{r}_j, \mathbf{r}', \omega\right) \cdot \hat{\mathbf{f}}(\mathbf{r}', \omega) \\
+ \hat{\mathbf{f}}^\dagger(\mathbf{r}', \omega) \cdot \overleftrightarrow{\mathbf{G}}_e^\dagger\left(\mathbf{r}_j, \mathbf{r}', \omega\right) \cdot \mathbf{d} \left(\hat{\sigma}_-^{(j)} e^{i\delta_-(t-\tau)}\right) \Bigg] \rho_A \otimes |\{0\}\rangle\langle\{0\}|
\end{aligned}
$$

and that this expression can be reduced keeping in mind (1) the fluctuation-dissipation relation in Eq. 3.0.18 [36] rewritten here for completeness,

$$
\int \mathrm{d}^3 r\, \overleftrightarrow{\mathbf{G}}_e\left(\mathbf{r}_1, \mathbf{r}, \omega\right) \cdot \overleftrightarrow{\mathbf{G}}_e^\dagger\left(\mathbf{r}_2, \mathbf{r}, \omega\right) = \frac{\hbar \mu_0 \omega^2}{\pi}\, \mathrm{Im}\, \overleftrightarrow{\mathbf{G}}\left(\mathbf{r}_1, \mathbf{r}_2, \omega\right), \qquad (3.0.18)
$$

and (2) the rotating-wave approximation, in which the fast phase δ_+ is averaged to zero

$$
\int_0^\infty \mathrm{d}\tau e^{-i\delta_+ \tau} = 0 \qquad (3.0.19)
$$

and where the slow phase δ_- give rise to

$$
\int_0^\infty \mathrm{d}\tau e^{-i\delta_- \tau} = \pi\delta(\omega - \omega_0) - i\mathcal{P}\frac{1}{\omega - \omega_0} \qquad (3.0.20)
$$

with $\mathcal{P}$ denoting the Cauchy principal value. With these facts we arrive at

$$
\begin{aligned}
(\mathrm{I}) = &- \frac{\mu_0 \omega_0^2}{\hbar} \sum_{i,j}^{N} \hat{\sigma}_+^{(i)} \hat{\sigma}_-^{(j)}\ \mathbf{d}^\dagger \cdot \mathrm{Im}\, \overleftrightarrow{\mathbf{G}}\left(\mathbf{r}_i, \mathbf{r}_j, \omega_0\right) \cdot \mathbf{d}\ \rho_A \\
&+ i\frac{\mu_0}{\hbar\pi} \sum_{i,j}^{N} \mathcal{P} \int d\omega \frac{\omega^2}{\omega - \omega_0} \hat{\sigma}_+^{(i)} \hat{\sigma}_-^{(j)}\ \mathbf{d}^\dagger \cdot \mathrm{Im}\, \overleftrightarrow{\mathbf{G}}\left(\mathbf{r}_i, \mathbf{r}_j, \omega_0\right) \cdot \mathbf{d}\ \rho_A. \qquad (3.0.21)
\end{aligned}
$$

The real and imaginary parts of the Green's function are not independent, they are

related via the Kramers-Krong relations [36, 41]:

$$\frac{1}{\pi}\mathcal{P}\int_{-\infty}^{\infty}\frac{\mathrm{d}\omega}{\omega-\omega_0}\omega^2\,\mathrm{Im}\overleftrightarrow{\mathbf{G}}\left(\boldsymbol{r}_m,\boldsymbol{r}_n,\omega\right)=\omega_0^2\,\mathrm{Re}\overleftrightarrow{\mathbf{G}}\left(\boldsymbol{r}_m,\boldsymbol{r}_n,\omega_0\right) \tag{3.0.22}$$

so finally,

$$\begin{aligned}(\mathrm{I})=&-\frac{\mu_0\omega_0^2}{\hbar}\sum_{i,j}^{N}\hat{\sigma}_+^{(i)}\hat{\sigma}_-^{(j)}\;\mathbf{d}^\dagger\cdot\mathrm{Im}\overleftrightarrow{\mathbf{G}}\left(\mathbf{r}_i,\mathbf{r}_j,\omega_0\right)\cdot\mathbf{d}\;\rho_A\\&+i\frac{\mu_0\omega_0^2}{\hbar}\sum_{i,j}^{N}\hat{\sigma}_+^{(i)}\hat{\sigma}_-^{(j)}\;\mathbf{d}^\dagger\cdot\mathrm{Re}\overleftrightarrow{\mathbf{G}}\left(\mathbf{r}_i,\mathbf{r}_j,\omega_0\right)\cdot\mathbf{d}\;\rho_A.\end{aligned} \tag{3.0.23}$$

The remaining terms of Eq. 7.1.1 can be worked in a similar way as exemplified with (I). Defining the dissipative and dispersive interactions between i^{th} and j^{th} atoms as

$$\Gamma_{ij}=2\left(\frac{\mu_0\omega_0^2}{\hbar}\right)\mathbf{d}^\dagger\cdot\mathrm{Im}\overleftrightarrow{\mathbf{G}}\left(\mathbf{r}_i,\mathbf{r}_j,\omega_0\right)\cdot\mathbf{d}, \tag{3.0.24}$$

$$J_{ij}=-\left(\frac{\mu_0\omega_0^2}{\hbar}\right)\mathbf{d}^\dagger\cdot\mathrm{Re}\overleftrightarrow{\mathbf{G}}\left(\mathbf{r}_i,\mathbf{r}_j,\omega_0\right)\cdot\mathbf{d}, \tag{3.0.25}$$

corresponding to the modification to the collective spontaneous emission and the level shifts respectively. Note that the Eq. 7.1.23 is in complete agreement with Eq. 2.5.12 in chapter 3. With this, we can finally add each of the four commutator contributions in Eq. 3.0.15 to obtain our Born-Markov master equation that describe the dynamics of the atomic internal degrees of freedom

$$\dot{\rho}_A=(\mathrm{I})+(\mathrm{II})+(\mathrm{III})+(\mathrm{IV})=-\frac{i}{\hbar}\left[H_A',\rho_A\right]+\mathcal{L}(\rho_A) \tag{3.0.26}$$

The modified Hamiltonian H_A' and the superoperator $\mathcal{L}(\rho_A)$ describe the coherent and the dissipative dynamics of the collective atomic system, and are given by

$$H_A'=\hbar\sum_{i,j}^{N}J_{ij}\hat{\sigma}_+^{(i)}\hat{\sigma}_-^{(j)} \tag{3.0.27}$$

and

$$\begin{aligned}\mathcal{L}(\rho_A) = &-\frac{1}{2}\left\{\sum_{i,j}^{N}\Gamma_{ij}\hat{\sigma}_+^{(i)}\hat{\sigma}_-^{(j)}\ ,\ \rho_A\right\}\\ &+\int d^3\mathbf{k}\left[\sum_{i}^{N}\int d^3r\frac{e^{i\mathbf{k}\cdot\mathbf{r}}}{2\pi\hbar}\hat{\sigma}_-^{(i)}\mathbf{d}\cdot\overleftrightarrow{\mathbf{G}}^{\dagger}\left(\mathbf{r}_i,\mathbf{r},\omega_0\right)\right]\ \rho_A\\ &\times\left[\sum_{j}^{N}\int d^3r'\frac{e^{-i\mathbf{k}\cdot\mathbf{r}'}}{2\pi\hbar}\hat{\sigma}_+^{(j)}\ \overleftrightarrow{\mathbf{G}}\left(\mathbf{r}_j,\mathbf{r}',\omega_0\right)\cdot\mathbf{d}^{\dagger}\right]\end{aligned} \tag{3.0.28}$$

respectively. The last term in the RHS has the well-known form $L\rho_A L$, which is valid for the case where the jump operator was not space-dependent. The dynamics under the master equation can analogously be described in the quantum jump formalism of open systems [38],

$$\dot{\rho}_A = -\frac{i}{\hbar}\left(H_{\text{eff}}\rho_A - \rho_A H_{\text{eff}}^{\dagger}\right) + \mathcal{L}'(\rho_A) \tag{3.0.29}$$

where the atomic wave function evolves deterministically under an effective non-Hermitian Hamiltonian that reads

$$H_{\text{eff}} = -\mu_0\omega_0^2\sum_{i,j}^{N}\mathbf{d}^{\dagger}\cdot\overleftrightarrow{\mathbf{G}}\left(\mathbf{r}_i,\mathbf{r}_j\right)\cdot\mathbf{d}\ \hat{\sigma}_+^{(i)}\hat{\sigma}_-^{(j)}. \tag{3.0.30}$$

and decays according to the term

$$\mathcal{L}'(\rho_A) = \mathcal{L}(\rho_A) + \frac{1}{2}\left\{\sum_{i,j}^{N}\Gamma_{ij}\hat{\sigma}_+^{(i)}\hat{\sigma}_-^{(j)}\ ,\ \rho_A\right\}. \tag{3.0.31}$$

3.1 Lindbland master equation on Heisenberg picture

The Lindbland equation in the Schrödinger picture Eq. 3.0.26 can be schematized as a linear superoperator on the density matrices

$$(\mathscr{L})_*\rho = -i[H,\rho] + \sum_m \left(L_m \rho L_m^\dagger - \frac{1}{2}\left\{ L_m^\dagger L_m, \rho \right\} \right). \tag{3.1.1}$$

It is possible to derive the Heisenberg picture Lindblad equation, which has the form [40]

$$\mathscr{L}_{\mathrm{H}} X = i[H,X] + \sum_m \left(L_m^\dagger X L_m - \frac{1}{2}\left\{ L_m^\dagger L_m, X \right\} \right) \tag{3.1.2}$$

where the superoperator $\mathscr{L}_{\mathrm{H}}$ acts in the operator space. To obtain the dynamics of the operators X we can modify the expression Eq. 3.0.26 to get

$$\dot{X} = \frac{i}{\hbar}\left[H'_A, X \right] + \mathscr{L}_{\mathrm{H}}(X) \tag{3.1.3}$$

with the dissipation given by

$$\begin{aligned} \mathscr{L}_{\mathrm{H}}(X) = &-\frac{1}{2}\left\{ \sum_{i,j}^{N} \Gamma_{ij} \hat{\sigma}_+^{(i)} \hat{\sigma}_-^{(j)} \ , \ X \right\} \\ &+ \int d^3\mathbf{k} \left[\sum_i^N \int d^3r \frac{e^{i\mathbf{k}\cdot\mathbf{r}}}{2\pi\hbar} \hat{\sigma}_+^{(i)} \mathbf{d}^\dagger \cdot \overleftrightarrow{\mathbf{G}}\left(\mathbf{r}_i, \mathbf{r}, \omega_0\right) \right] X \\ &\times \left[\sum_j^N \int d^3r' \frac{e^{-i\mathbf{k}\cdot\mathbf{r}'}}{2\pi\hbar} \hat{\sigma}_-^{(j)} \ \overleftrightarrow{\mathbf{G}}^\dagger \left(\mathbf{r}_j, \mathbf{r}', \omega_0\right) \cdot \mathbf{d} \right]. \end{aligned} \tag{3.1.4}$$

To fit with the expression in Eq.3.1.2, , it is necessary to explicitly clarify the jump operators

$$L_m = \int \mathbf{d}^3 r \frac{\mathbf{e^{-ik\cdot r}}}{2\pi\hbar} \sigma_-^m \ \overleftrightarrow{\mathbf{G}}^\dagger \left(\mathbf{r}_i, \mathbf{r}, \omega_0\right) \cdot \mathbf{d} \tag{3.1.5}$$

which satisfy

$$\int d^3\mathbf{k} \sum_m \hat{L}_m^\dagger \hat{L}_m = \sum_{m,n=1}^{N} \Gamma_{mn} \sigma_+^{(m)} \sigma_-^{(n)}. \tag{3.1.6}$$

It is important to highlight that the derivation was considering only the resonant part only, which depends on the direct response of the atom with the electric field at the frequency ω_0, while the off-resonant part depends on the broadband frequency response of the environment. These effects were neglected since the off-resonant contributions from virtual photons at second-order scale as $\sim 1/r^3$, and those at fourth-order that scale as $\sim 1/r^6$. The predominant contribution for the lens system is the resonant dipole-dipole interaction, which scales as $\sim 1/r$.

Chapter 4

A Point Spread Function for the Lens

The framework of Green's functions allows to modify the geometry of the space in which the radiation propagates. In this study we want to study the effect of photon exchange between two widely separated groups of atoms. To highlight the dipole-dipole interaction as the main responsible for the physical effects of this research, it will be required a reciprocal interaction of the emitting objects on both sides of the lens, in such a way that the number of photons captured on both sides of the lens are the same. So we look for a Green's function for an aplanatic lens with both focal length equal. An aplanatic lens is generally composed of two or three lenses such that spherical and coma aberrations are suppressed [42]. Enderlein [25] proposed a useful method for obtaining the in-plane image of a small emitting object through a series of converging lenses in order to relate the resolving power to the aperture of a microscope [28]. The field strength in the image plane given by an elementary emitting object, a dipole, is given by Green's dyadic function due to a point source, called in this context point spread function. This mechanism can also be used as a basis for the derivation of a dyadic Green's function for an aplanatic lens that meets the requirement of having both focal lengths equal. The treatment used for this purpose restricts the position of these atoms only in the focal zone of the optical system.

For the derivation of an appropriate Green's function, we will follow the propagation numbering in Fig. 4.0.1. In the first step (Fig. 4.0.1(1)) we will assume the absence of the lens, so the dipole emits virtual and real photons, as shown in Eq.

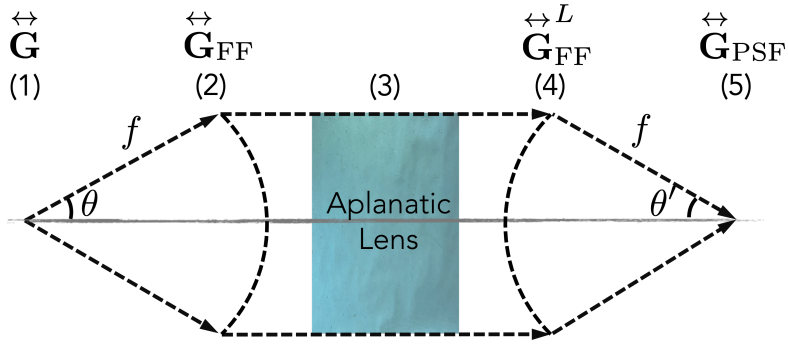

Figure 4.0.1: Optical system showing the five stages of propagation. First (1), there are a dipole emitting near and far fields. At the distance f (2) only far-field is captured. An aplanatic lens can be modeled with two reference spheres of radius f. Between both spheres the field propagates collimated (3). Just after the second (4) reference sphere the field is given by the far-field Green function with the opposite sign. Using Eq.**??**, it's possible to find focal field (5) in cylindrical coordinates (ρ, φ, z). These coordinates are shown more clearly in following figure.

2.4.14, with all the components (G_{NF}), (G_{IF}) and (G_{FF}), generating an electric field as seen in Eq. 2.4.9. The distribution of energy radiated by the dipole depends on the scale in question [43], but for our case of an aplanatic lens focal length much greater than the wavelength of the emitted photons, $f \gg \lambda$, only the far-field term will contribute. It is convenient for the course of the chapter to write (G_{FF}) in cylindrical coordinates:

$$\overleftrightarrow{\mathbf{G}}_{\mathrm{FF}}(\mathbf{r}, 0, \omega) = \frac{\exp(\mathrm{i}\omega r/c)}{4\pi r} \times \begin{bmatrix} 1-\cos^2\phi\sin^2\theta & -\sin\phi\cos\phi\sin^2\theta & -\cos\phi\sin\theta\cos\theta \\ -\sin\phi\cos\phi\sin^2\theta & 1-\sin^2\phi\sin^2\theta & -\sin\phi\sin\theta\cos\theta \\ -\cos\phi\sin\theta\cos\theta & -\sin\phi\sin\theta\cos\theta & \sin^2\theta \end{bmatrix}. \tag{4.0.1}$$

Note that the emitter is assumed to be at the origin of coordinates, which in this case is the left focus of Fig. 4.0.1. The position of the atom at the far right focal zone of the optical system is given by the vector $\mathbf{r}$, whose coordinate origin is at the right focus, not the left.

As already said, just before the first reference sphere (Fig. 4.0.1(2)) only the far field radiation (G_{FF}) will survive, since the others decay faster than $1/r$. Assuming

that the reflection indices of the components of the optical system are negligible, we can think that all the radiative content is collimated between the two reference spheres (Fig. 4.0.1 (3)), travelling as plane waves. Therefore, just after the second reference sphere (Fig. 4.0.1(4)), and for a non-reflective aplanatic lens, the electric field at position $\mathbf{r}$ (to the right of the frame) produced by a dipole (at the focus of the left side left), can be written as

$$\mathbf{E}_{(4)}(\mathbf{r}) = -\omega^2 \mu_0 \overleftrightarrow{\mathbf{G}}_{\mathrm{FF}}(\mathbf{r}, 0, \omega)\, \mathbf{p}_0 \tag{4.0.2}$$

where ω is the characteristic angular frequency of the atomic transition and a non-magnetic media is assumed. As seems intuitive, the far field $\mathbf{E}_{(4)}$ can be thought of in the opposite way to that of a dipole emitting divergent radiation. The field is focused down, in the direction of the focus on the right.

But our goal is to compute the focal fields (4.0.1(5)), that is, the field in the region near the focus on the right. Our starting point is Eq. 2.2.9 that relates the electric fields to the Fourier components. For a radiation inwards the focus of the second reference sphere,

$$\mathbf{E}(x, y, z) = \int_{k_x^2 + k_y^2 < k_{\max}^2} \mathrm{e}^{\mathrm{i}[k_x x + k_y y - k_z z]} \hat{\mathbf{E}}_0(k_x, k_y)\, \mathrm{d}k_x \mathrm{d}k_y \tag{4.0.3}$$

with cutoff wavenumber $k_{\max}$ determined by the maximum aperture angle $\theta_{\max}$. We can combine this with the expression for far-field Eq. 2.2.11 to get the Eq. 2.2.12, rewritten here for convenience

$$\mathbf{E}(x, y, z) = \frac{\mathrm{i} r \mathrm{e}^{-\mathrm{i}kr}}{2\pi} \int_{k_x^2 + k_y^2 < k_{\max}^2} \mathbf{E}_\infty\left(\frac{k_x}{k}, \frac{k_y}{k}\right) \mathrm{e}^{\mathrm{i}[k_x x + k_y y \pm k_z z]} \frac{1}{k_z}\, \mathrm{d}k_x\, \mathrm{d}k_y, \tag{4.0.4}$$

To proceed further, we perform two coordinate transformations animated by the geometry of the second reference sphere. These expressions are integrals over k-space, so we can introduce spherical coordinates with

$$k_x = k \sin\theta \cos\phi, \quad k_y = k \sin\theta \sin\phi, \quad k_z = k \cos\theta \tag{4.0.5}$$

and a two-dimensional Jacobian to transform the integrating factor $\mathrm{d}k_x \mathrm{d}k_y$ to one

suitable to the new coordinates,

$$J = \begin{vmatrix} \frac{\partial k_x}{\partial \theta} & \frac{\partial k_x}{\partial \phi} \\ \frac{\partial k_y}{\partial \theta} & \frac{\partial k_y}{\partial \phi} \end{vmatrix} = \begin{vmatrix} k\cos\theta\cos\phi & -k\sin\theta\sin\phi \\ k\cos\theta\sin\phi & k\sin\theta\cos\phi \end{vmatrix} = k^2\sin\theta\cos\theta. \tag{4.0.6}$$

Thus, $k_z^{-1}\mathrm{d}k_x\mathrm{d}k_y = k\sin\theta\mathrm{d}\theta\mathrm{d}\phi$. For the focus positions, we finally switch to cylinder coordinates with $(x, y, z) = (\rho\cos\varphi, \rho\sin\varphi, z)$. With this, we can reexpress the term in the exponential of Eq. 4.0.4 as

$$k_x x + k_y y = k\sin\theta\cos\phi\rho\cos\varphi + k\sin\theta\sin\phi\rho\sin\varphi = k\rho\sin\theta\cos(\phi-\varphi). \tag{4.0.7}$$

These coordinate transformations allow us rewriting Eq. 4.0.4 in the form

$$\mathbf{E}(\rho,\varphi,z) = -\frac{\mathrm{i}kf\mathrm{e}^{-\mathrm{i}kf}}{2\pi}\int_0^{\theta_{\max}}\int_0^{2\pi}\mathbf{E}_\infty(\theta,\phi)\mathrm{e}^{\mathrm{i}kz\cos\theta}\mathrm{e}^{\mathrm{i}k\rho\sin\theta\cos(\phi-\varphi)}\sin\theta\mathrm{d}\phi\mathrm{d}\theta \tag{4.0.8}$$

where $\theta_{\max}$ is the opening angle of the lens. The distance r between the focal point and the surface of the reference sphere has been replaced by the focal length f of the lens. This result allows us to calculate the focusing of an arbitrary optical field $\mathbf{E}_\infty$ by an aplanatic lens with focal length f and numerical aperture $\mathrm{NA} = n\sin\theta_{\max}$, where $(0 < \theta_{\max} < \pi/2)$. For this work, a homogeneous environment is assumed, so the refractive index outside the lens can be set to $n \approx 1$. The final step is to replace the incoming far fields $\mathbf{E}_\infty$ with those after crossing the Gaussian reference sphere, $\mathbf{E}_{(4)}$. This task must be carried out meticulously term by term. For clarity, the expression that results after that replacement can be expanded as

$$\begin{aligned}\mathbf{E}_{\mathrm{fo}}(\rho,\varphi,z) =& \frac{\omega^2}{\varepsilon_0 c^2}\left\{\frac{\mathrm{i}kf\mathrm{e}^{-\mathrm{i}kf}}{2\pi}\frac{e^{\mathrm{i}kf}}{4\pi f}\int_0^{\theta_{\max}}\int_0^{2\pi}\right. \\ &\left.\times\ \overleftrightarrow{\mathbf{g}}\,\mathrm{e}^{\mathrm{i}kz\cos\theta}\mathrm{e}^{\mathrm{i}k\rho\sin\theta\cos(\phi-\varphi)}\sin\theta\mathrm{d}\phi\mathrm{d}\theta\right\}\cdot\mathbf{p}\end{aligned} \tag{4.0.9}$$

where $\overleftrightarrow{\mathbf{g}}$ is the matrix

$$\overleftrightarrow{\mathbf{g}} = \begin{bmatrix} 1-\cos^2\phi\sin^2\theta & -\sin\phi\cos\phi\sin^2\theta & -\cos\phi\sin\theta\cos\theta \\ -\sin\phi\cos\phi\sin^2\theta & 1-\sin^2\phi\sin^2\theta & -\sin\phi\sin\theta\cos\theta \\ -\cos\phi\sin\theta\cos\theta & -\sin\phi\sin\theta\cos\theta & \sin^2\theta \end{bmatrix} \tag{4.0.10}$$

The term in curly brackets will be our new point-spread function of the optical system,

$$\overleftrightarrow{\mathbf{G}}_{\mathrm{PSF}}= \frac{\mathrm{i}k}{8\pi^2}\int_0^{\theta_{\max}}\int_0^{2\pi} \overleftrightarrow{\mathbf{g}}\ \ \mathrm{e}^{\mathrm{i}kz\cos\theta}\mathrm{e}^{\mathrm{i}k\rho\sin\theta\cos(\phi-\varphi)}\sin\theta \mathrm{d}\phi\mathrm{d}\theta \tag{4.0.11}$$

The integrals over the azimuthal angle ϕ can be performed analytically using the identities [43]

$$\int_0^{2\pi}\left\{\begin{array}{c}\sin n\phi\\ \cos n\phi\end{array}\right\} e^{ix\cos(\phi-\varphi)}d\phi = 2\pi i^n J_n(x)\left\{\begin{array}{c}\sin n\varphi\\ \cos n\varphi\end{array}\right\} \tag{4.0.12}$$

where J_n are the Bessel functions of order n. The remaining integrand, over the polar angle θ, will have exponentials of the form

$$\mathrm{e}^{\mathrm{i}kr}\mathrm{e}^{\mathrm{i}kz\cos\theta}\mathrm{e}^{\mathrm{i}k\rho\sin\theta\cos(\phi-\varphi)} \tag{4.0.13}$$

which are prefactors for the matrix elements g_{ii} of Eq. 4.0.10, and that both multiplied give us the elements of the new point spread function of the system. The replacements of each element of g_{ii} that build $\overleftrightarrow{\mathbf{G}}_{\mathrm{PSF}}$ with their respective integrals are detailed in the appendices chapter, section 7.2. The point spread function that gives us the electric field to the right of the system of an aplanatic lens of both focal lengths due to the emission of real photons by a dipole at the left focus of the system is given by

$$\overleftrightarrow{\mathbf{G}}_{\mathrm{PSF}}\ (\mathbf{r},0)\ = \frac{\mathrm{i}k}{8\pi}\left[\begin{array}{ccc} I_1+I_2\cos(2\varphi) & I_2\sin(2\varphi) & -2\mathrm{i}I_3\cos\varphi\\ I_2\sin(2\varphi) & I_1-I_2\cos(2\varphi) & -2\mathrm{i}I_3\sin\varphi\\ -2\mathrm{i}I_3\cos\varphi & -2\mathrm{i}I_3\sin\varphi & 2I_4\end{array}\right] \tag{4.0.14}$$

where the measurement position r = (ρ,φ,z) is in cylindrical coordinates and the integrals I_1-I_4 are a specific case of a general one shown in Eqs 4.2.4-4.2.7.

4.1 Generalizing the Green function

The far-field Green's function in free space Eq.4.0.1, only account for a dipole in the origin of the coordinate system, but we can change the term $r = |\mathbf{r} - \mathbf{r}_0|$ in the argument of the exponential, moving the position of the emitter an amount $\mathbf{r}_0 = (x_0, y_0, z_0)$ from the left origin,

$$r \quad \longrightarrow \quad r - \left(x_0 \frac{x}{r} + y_0 \frac{y}{r} + z_0 \frac{z}{r} \right). \tag{4.1.1}$$

This replacement gives us

$$\begin{aligned} \overleftrightarrow{\mathbf{G}}_{\mathrm{PSF}}(\mathbf{r}, \mathbf{r}_0) = & \frac{\exp(\mathrm{i}kr)}{4\pi r} \exp\left[-\mathrm{i}k\left(x_0 x/r + y_0 y/r + z_0 z/r\right)\right] \\ & \times \begin{bmatrix} 1 - \cos^2\phi \sin^2\theta & -\sin\phi\cos\phi\sin^2\theta & -\cos\phi\sin\theta\cos\theta \\ -\sin\phi\cos\phi\sin^2\theta & 1 - \sin^2\phi\sin^2\theta & -\sin\phi\sin\theta\cos\theta \\ -\cos\phi\sin\theta\cos\theta & -\sin\phi\sin\theta\cos\theta & \sin^2\theta \end{bmatrix}. \end{aligned} \tag{4.1.2}$$

Writing the factors x/r, y/r and z/r in spherical coordinates, we get an exponential of the type

$$\exp\left[-\mathrm{i}kr\left(x_0\cos\phi\sin\theta + y_0\sin\phi\sin\theta + z_0\cos\theta\right)\right], \tag{4.1.3}$$

which must multiplying the integrands of the expression Eq. 4.0.11. In compact notation, the integrals I_1-I_4 can be written as

$$I_{mn}(\mathbf{r}, 0) = \int_0^{\theta_{\max}} \mathrm{e}^{\mathrm{i}kz\cos\theta} \sin\theta \int_0^{2\pi} \left(\overleftrightarrow{\mathbf{G}}_0 \right)_{mn} (\mathbf{r}, 0)\ \mathrm{e}^{\mathrm{i}k\sin\theta\rho\cos(\phi-\varphi)}\ \mathrm{d}\phi\mathrm{d}\theta. \tag{4.1.4}$$

where the subscripts $m, n = \{1, 2, 3\}$ indicate the element of Green's function in free-space Eq. 4.0.1. This expression can be generalized to allow the emitter to be at any position within the left focal zone by writing

$$\begin{aligned} I_{mn}(\mathbf{r}, \mathbf{r}_0) \ = \ & \int_0^{\theta_{\max}} e^{ik\cos\theta(z-z_0)} \sin\theta \\ & \times \int_0^{2\pi} \left(\overleftrightarrow{\mathbf{G}}_0 \right)_{mn} (\mathbf{r}, \mathbf{r}_0)\ \mathrm{e}^{\mathrm{i}k\sin\theta\{x_\rho\cos\phi + y_\rho\sin\phi\}} e^{-\mathrm{i}k\sin\theta\{x_0\cos\phi + y_0\sin\phi\}}\ \mathrm{d}\phi\mathrm{d}\theta \end{aligned} \tag{4.1.5}$$

where we have used

$$\begin{aligned}\rho\cos(\phi-\varphi) &= \frac{\rho}{2}\left[^{-\mathrm{i}\varphi}e^{\mathrm{i}\phi}+e^{\mathrm{i}\varphi}e^{-\mathrm{i}\phi}\right] \\ &= x_\rho\cos\phi+y_\rho\sin\phi \end{aligned} \tag{4.1.6}$$

with $x_\rho=\rho\cos\varphi$ and $y_\rho=\rho\sin\varphi$. Thus, in the integral over ϕ we have exponentials whose arguments can be rewritten as

$$[x_\rho\cos\phi+y_\rho\sin\phi]-[x_0\cos\phi+y_0\sin\phi] = \rho_{\mathrm{eff}}\cos(\phi-\varphi_{\mathrm{eff}}) \tag{4.1.7}$$

where

$$\rho_{\mathrm{eff}}=\sqrt{(x_\rho-x_0)^2+(y_\rho-y_0)^2} \quad \varphi_{\mathrm{eff}}=\begin{cases}\tan^{-1}\frac{y_{\mathrm{eff}}}{x_{\mathrm{eff}}} & x_{\mathrm{eff}}>0\\ \tan^{-1}\frac{y_{\mathrm{eff}}}{x_{\mathrm{eff}}}+\pi & x_{\mathrm{eff}}<0\end{cases} \quad z_{\mathrm{eff}}=z-z_0 \tag{4.1.8}$$

are effective cylindrical coordinates between the atoms at opposite ends of the lens, and are the input coordinates to obtain the integrals of the matrix elements of $\overleftrightarrow{\mathbf{G}}_{\mathrm{PSF}}$ for an emitter atom with position $\mathbf{r}_0$ and a receiver atom with position $\mathbf{r}$,

$$I_{mn}(\mathbf{r},\mathbf{r}_0)=\int_0^{\theta_{\max}}e^{\mathrm{i}kz_{\mathrm{eff}}\cos\theta}\sin\theta\int_0^{2\pi}\left(\overleftrightarrow{\mathbf{G}}_0\right)_{mn}(\mathbf{r},\mathbf{r}_0)e^{\mathrm{i}k\sin\theta\rho_{\mathrm{eff}}\cos(\phi-\varphi_{\mathrm{eff}})}\,\mathrm{d}\phi\mathrm{d}\theta. \tag{4.1.9}$$

It is important to highlight that these coordinates indicate that within the focal zones the intensity of the field only matters the effective distance between the atom on the right and the one on the left. Absolute coordinates have no role in determining field strength. This is true in the region where the focal field can be written as Eq.4.0.8. Beyond that region, the field is not given by integrals like Eq.4.1.9 anymore.

4.2 Final remarks

One last consideration comes from the study of exchanging the position of the emitter and receiver, which changes both the relative distance $z_{\mathrm{eff}}\rightarrow -z_{\mathrm{eff}}$ and the direction of propagation $k_z\rightarrow -k_z$. This shows that under exchange of atoms there

is no alteration in the arguments of the integral.

$$I(\mathbf{r},\mathbf{r}_0) \propto \mathrm{e}^{ik_z\ z_{\mathrm{eff}}} \longrightarrow I(\mathbf{r}_0,\mathbf{r}) \propto \mathrm{e}^{ik_z\ z_{\mathrm{eff}}}. \tag{4.2.1}$$

This is equivalent to have the absolute value $|z_{\mathrm{eff}}|$ in the argument.

$$I \propto \mathrm{e}^{ik_z\ |z_{\mathrm{eff}}|}. \tag{4.2.2}$$

In this way, we obtain the dyadic point spread function that gives the electric field felt by j^{th} atom product of the radiation emitted by the i^{th} atom at the other end of the lens,

$$\overleftrightarrow{\mathbf{G}}_{\mathrm{PSF}}\ (\mathbf{r}_i,\mathbf{r}_j) = \frac{\mathrm{i}k}{8\pi}\begin{bmatrix} I_1 + I_2\cos(2\varphi_{ij}) & I_2\sin(2\varphi_{ij}) & -2\mathrm{i}I_3\cos\varphi_{ij} \\ I_2\sin(2\varphi_{ij}) & I_1 - I_2\cos(2\varphi_{ij}) & -2\mathrm{i}I_3\sin\varphi_{ij} \\ -2\mathrm{i}I_3\cos\varphi_{ij} & -2\mathrm{i}I_3\sin\varphi_{ij} & 2I_4 \end{bmatrix}, \tag{4.2.3}$$

and its matrix elements

$$I_1(\mathbf{r}_i,\mathbf{r}_j) = \int_0^{\theta_{\max}} \sin\theta\{1+\cos^2\theta\}e^{ik_z|z_{ij}|}J_0(k\sin\theta\rho_{ij})\ \mathrm{d}\theta \tag{4.2.4}$$

$$I_2(\mathbf{r}_i,\mathbf{r}_j) = \int_0^{\theta_{\max}} \sin\theta\{1-\cos^2\theta\}e^{ik_z|z_{ij}|}J_2(k\sin\theta\rho_{ij})\ \mathrm{d}\theta \tag{4.2.5}$$

$$I_3(\mathbf{r}_i,\mathbf{r}_j) = \int_0^{\theta_{\max}} \sin^2\theta\cos\theta e^{ik_z|z_{ij}|}J_1(k\sin\theta\rho_{ij})\ \mathrm{d}\theta \tag{4.2.6}$$

$$I_4(\mathbf{r}_i,\mathbf{r}_j) = \int_0^{\theta_{\max}} \sin^3\theta e^{ik_z|z_{ij}|}J_0(k\sin\theta\rho_{ij})\ \mathrm{d}\theta \tag{4.2.7}$$

where the effective coordinates relating the positions $\mathbf{r}_i = (x_0, y_0, z_0)$ and $\mathbf{r}_j = (x_\rho, y_\rho, z_\rho)$ are given in Eq. 4.1.8. The change from absolute to relative perspective and the symmetry under exchange of atoms is evidenced in the fulfillment of the Onsager reciprocity for symmetric tensors

$$\overleftrightarrow{\mathbf{G}}_{\mathrm{PSF}}\ (\mathbf{r}_i,\mathbf{r}_j,\omega) = \overleftrightarrow{\mathbf{G}}_{\mathrm{PSF}}\ (\mathbf{r}_j,\mathbf{r}_i,\omega)\,, \tag{4.2.8}$$

and the Schwarz reflection principle [39],

$$\overleftrightarrow{\mathbf{G}}^{*}_{\mathrm{PSF}}\ (\mathbf{r}_i, \mathbf{r}_j, \omega) = \overleftrightarrow{\mathbf{G}}_{\mathrm{PSF}}\ (\mathbf{r}_i, \mathbf{r}_j, -\omega^*)\,. \tag{4.2.9}$$

Furthermore, as shown in Fig. 5.0.2, the condition $\overleftrightarrow{\mathbf{G}}_{\mathrm{PSF}}\ (\mathbf{r}_i, \mathbf{r}_j, \omega) \to 0$ as $|\mathbf{r}_i - \mathbf{r}_j| \to \infty$ is fulfilled.

Chapter 5

Dipole-Dipole Interaction through a Lens

For a concise study of the dipole-dipole interaction mediated by an aplanatic lens we will start by considering a system of two atoms of two levels, A1 and A2, which will be separated by an aplanatic lens, as shown in Fig. 5.0.1.

In order for atoms to be described as a two-level system, we need a cyclic atomic transition between hyperfine states of some alkaline element. In particular, let us consider the $6^2\ S_{1/2} \longrightarrow 6^2P_{3/2}$ transition of ^{133}Cesium atoms. In order to set explicit ground and excited states for future reference, we can write

$$|g\rangle = |J = 1/2, F = 4, m_F = \pm 4\rangle \longrightarrow |e\rangle = |J = 3/2, F = 5, m_F = \pm 5\rangle \quad (5.0.1)$$

as the cyclic transition with the matrix transition element $\langle J = 1/2 \| e\mathbf{r} \| J' = 3/2\rangle = 3.8 \times 10^{-29}$ C$\cdot$m, and transition rate $\gamma_0 = 2\pi \cdot 5.23$ MHz. By conservation of angular momentum, this transition emits circularly polarized photons (either σ^+ or σ^- light) of wavelength $\lambda_0 = 852$ nm. As seen in Eq. 2.5.13,

$$\left|\mathbf{d}_{(m_F=\pm 4 \to m_{F'}=\pm 5)}\right|^2 = \frac{2J+1}{2J'+1} \left|\langle J = 1/2 \| e\mathrm{d} \| J' = 3/2\rangle\right|^2, \quad (5.0.2)$$

should be considered. Therefore

$$\mathbf{d}_{(m_F=\pm 4 \to m_{F'}=\pm 5)} = 2.6880(34) \times 10^{-29} \mathrm{C} \cdot \mathrm{m}. \quad (5.0.3)$$

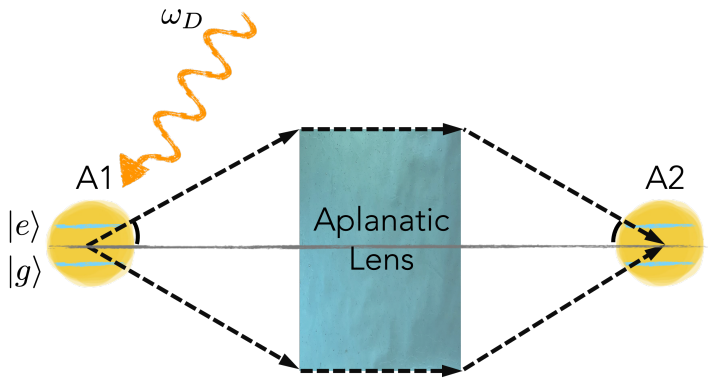

Figure 5.0.1: Schematic representation of two two-level atoms, A1 and A2, interacting with each other via an aplanatic lens with f as the focal length. The atoms are placed at the two focal points of the optical system. Each atom has a resonance frequency of ω_0 and is weakly driven by a laser of frequency ω_D.

is the dipole moment for this transition [37].

The atoms A1 and A2 are placed near the focal points on each side of the lens, so they share photons mediated by $\overleftrightarrow{\mathbf{G}}_{\mathrm{PSF}}\left(\mathrm{r}_1, \mathrm{r}_2, \omega_D\right)$. The system exhibits azimuthal symmetry, that can be broken by the polarization of the atomic dipoles deviating from the optical axis. A homogeneous environment is assumed, so the refractive index outside the lens can be set to $n \approx 1$. We further assume that the atoms are weakly driven by a classical field of frequency ω_D. As seen in the chapter 4, the field that is reflected from or transmitted through inhomogeneities in the environment is given by the scattering Green's function, so the complete dynamics for an atom in the focal zone is given by

$$\overleftrightarrow{\mathbf{G}}^{A_n}_{\mathrm{tot}}\left(\mathbf{r}_1, \mathbf{r}_2, \omega_D\right) = \overleftrightarrow{\mathbf{G}}^{A_n}_{0}\left(\mathbf{r}_1, \mathbf{r}_2, \omega_D\right) + \overleftrightarrow{\mathbf{G}}_{\mathrm{PSF}}\left(\mathbf{r}_1, \mathbf{r}_2, \omega_D\right) \tag{5.0.4}$$

where $\mathbf{r}_1$ and $\mathbf{r}_1$ are inside the focal zone of their respective focus. This means that for an atom A_n the transition rate will be the usual one in free-space, plus a modification product of the resonant dipole-dipole interaction. The enhancement of emission and collective behavior is due to the scattering term $\overleftrightarrow{\mathbf{G}}_{\mathrm{S}} = \overleftrightarrow{\mathbf{G}}_{\mathrm{PSF}}$. From Eq. 2.5.12 we can calculate the modified transition rate

$$\Gamma_{12}(\omega_D) = \gamma_D \frac{6\pi c}{\omega_D} |\mathbf{d}_{m_F \to m_{F'}}|^2 \mathbf{n}_1 \cdot \mathrm{Im}\, \overleftrightarrow{\mathbf{G}}_{\mathrm{PSF}}\left(\mathbf{r}_1, \mathbf{r}_2, \omega_D\right) \cdot \mathbf{n}_2 \tag{5.0.5}$$

where the unit vectors $\mathbf{n}_a$ correspond to the orientation of the atomic dipole a. Also we have write for simplicity $\mathbf{d}_{m_F \to m_{F'}}$ instead of $\mathbf{d}_{(m_F=\pm 4 \to m_F=\pm 5)}$, and

$$\gamma_D = \frac{|\mathbf{d}|^2 \omega_D^3}{3\pi\hbar\epsilon_0 c^3} \tag{5.0.6}$$

is the emission rate for a dipole radiating at the drive frequency ω_D. When the drive detuning $\delta_D = \omega_0 - \omega_D$ is zero, the free-space transition rate γ_0 is recovered. The modification to the level shifts is given by

$$J_{12}(\omega_D) = -\gamma_D \frac{3\pi c}{\omega_D} |\mathbf{d}_{m_F \to m_{F'}}|^2 \mathbf{n}_1 \cdot \mathrm{Re}\, \overleftrightarrow{\mathbf{G}}_{\mathrm{PSF}}\, (\mathbf{r}_1, \mathbf{r}_2, \omega_D) \cdot \mathbf{n}_2. \tag{5.0.7}$$

Figure 5.0.2 shows the a cross section in the $xz-$plane of the spatial dependence of Γ_{12} (a) and J_{12} (b) for dipoles with orthogonal and parallel orientation with respect to the $z-$axis, evidencing a lensing effect within the focal zone of approximately $10\lambda_D$ in length, for a high NA lens. The fringes correspond to constructive and destructive interference effects in the collective behaviour, leading to super and sub radiant dissipation. This evidences the enhancement of the dipole-dipole interactions due to photons shared between both atoms.

The contribution of the lens to the enhancement of the dipole-dipole interactions can be better characterized by the modification to the spontaneous emission rate due to the collective decays Γ_{12}. The enhancement in the emission rate of one atom A1 at the focus $\mathbf{r}_1 = \mathbf{0}_1$ product of the radiation of the other atom A2 at the opposite focus $\mathbf{r}_2 = \mathbf{0}_2$ driven by an external field for an aperture NA≈ 0.866 (which correspond to an aperture of $\theta_{\max} = \pi/3$) will depend on the atomic state in which they are found, and is given by $\Gamma_{\mathrm{tot}} = \gamma_0 + \Gamma_{12}(\mathbf{0}_1, \mathbf{0}_2, \omega_D)\chi$, where χ is a non trivial function of the atomic state. In what follows it will not be necessary to write it explicitly. For an optimal state, the enhancement can be of the order $\Gamma_{\mathrm{tot}} \approx 1.55\gamma_0$.

Figure 5.0.3 shows the maximum dissipative dipole-dipole coupling $\Gamma_{12}^{\max}$ as a function of the aperture NA for two orthogonal orientations of the atomic dipole. We see that for a feasibly high NA and the correct atomic dipole alignment, the dipole-dipole interaction rate can reach near to a 60% of the bare atomic decay rate, with an approximately lineal dependence on the NA.

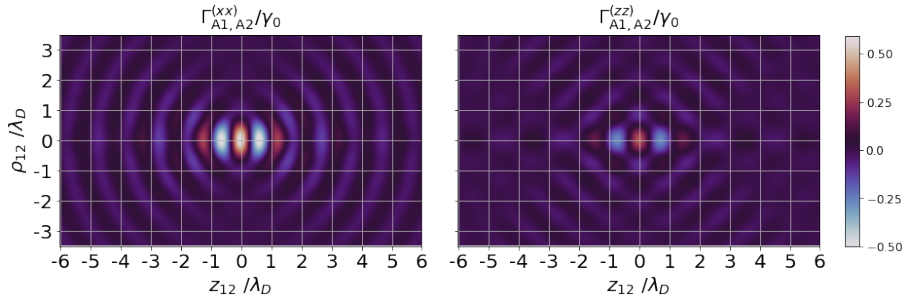

(a) Dissipative interaction $\Gamma_{\mathrm{A1,A2}} \equiv \Gamma_{12}$ for orthogonal (left) and parallel (right) orientation with respect to the $z-$axis, in units of γ_0.

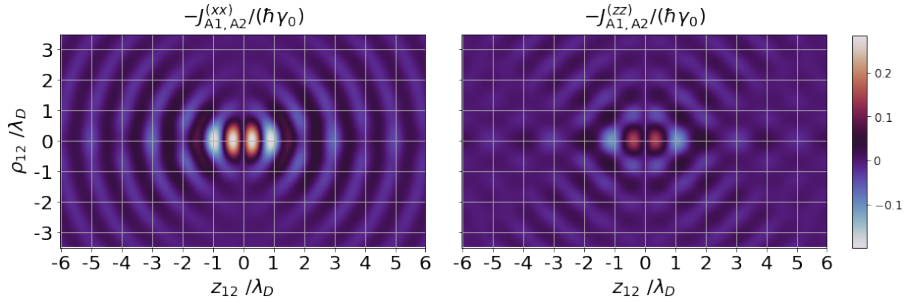

(b) Dispersive interaction $-J_{\mathrm{A1,A2}} \equiv -J_{12}$ for orthogonal (left) and parallel (right) orientation with respect to the $z-$axis, in units of $\hbar\gamma_0$.

Figure 5.0.2: Spatial distribution of the dissipative (a) and dispersive (b) interaction in the $xz-$ plane. The presence of an atom A1 emitting radiation produces a lens effect field in the focal zone at the opposite end. A second atom A2 at this end will be subject to dispersive and dissipative interactions depending on the relative positions and orientations between them, as is shown in the figures above, which are longitudinal sections for $\rho \in [0, 3.5\lambda_D]$ and $z \in [-6\lambda_D, 6\lambda_D]$, evidencing zones of minimum every $\sim \lambda_D$ for a NA$= 0.866$ (correspondig to $\theta_{\max} = \pi/3$ for $n \approx 1$), close to the state-of-the-art optical elements.

To position the atoms at the focus, they can be manipulated using red-detuned optical tweezers. These types of traps with $\Delta \gg 0$ create a negative dipole potential that attracts the atom into the light field, so the minimum potential are therefore found at positions with maximum intensity [44]. These optical dipole traps usually use large detunings and high intensities to keep the scattering rate as low as possible at a certain potential depth, since dipole potential scales as I/Δ, whereas the scattering rate scales as I/Δ^2.

Until now, the dynamics and the interaction between the atoms is completely

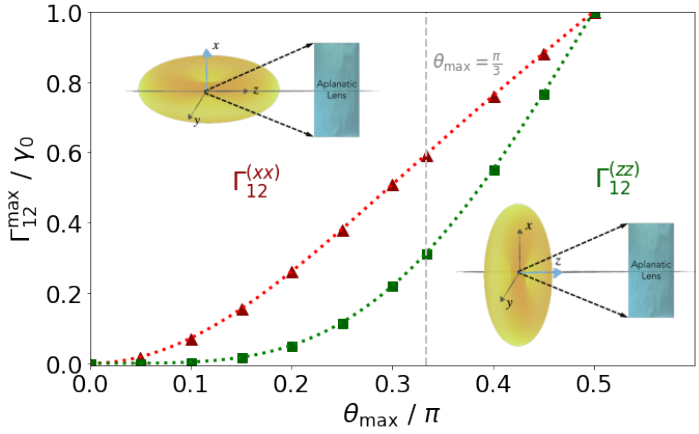

Figure 5.0.3: Maximum dissipative dipole-dipole coupling ($\Gamma_{12}^{\max}$) as a function of the angular aperture $\theta_{\max}$. The red (green) dotted curve represents $\Gamma_{12}^{\max}$ for two $x(z)$-oriented dipoles, as illustrated in the schematic inset figures. The dashed vertical line indicates an angular aperture of $\theta_{\max} \approx \pi/3$, where $\Gamma_{12}^{\max} \approx 0.6\Gamma_D$.

symmetrical, where each atom is subject to the electric field produced by the other atom and therefore experiences the modification to the collective spontaneous emission and the level shifts shown in Figure 5.0.2. Now, if we rotate the system as in Fig. 5.0.4 such that the gravity is parallel to the optic axis and then turn off the optical tweezer of the atom at the bottom, we can compare the CP force at distance with gravity and thus begin the study of a trapping mechanism due only to the well potential produced by the group of atoms on the top and mediated by the lens.

The total modified interaction Hamiltonian $H'_{A,\text{tot}}$, that is, the one that accounts for the interaction of the atoms at one end due to the radiation emitted at the other end and vice versa, is given by

$$H'_{A,\text{tot}} = \hbar \sum_{i,j}^{N} J_{ij} \left(\hat{\sigma}_+^{(i)} \hat{\sigma}_-^{(j)} + \hat{\sigma}_+^{(j)} \hat{\sigma}_-^{(i)} \right), \tag{5.0.8}$$

or from a compact point of view

$$H'_{A,\text{tot}} = H'_{A,(i)\to(j)} + H'_{A,(j)\to(i)} \tag{5.0.9}$$

where $H'_{A,(i)\to(j)}$ accounts for the interaction between the (i^{th}) atom in one end of the lens and the radiation generated by the (j^{th}) atom at the other end. $H'_{A,(j)\to(i)}$

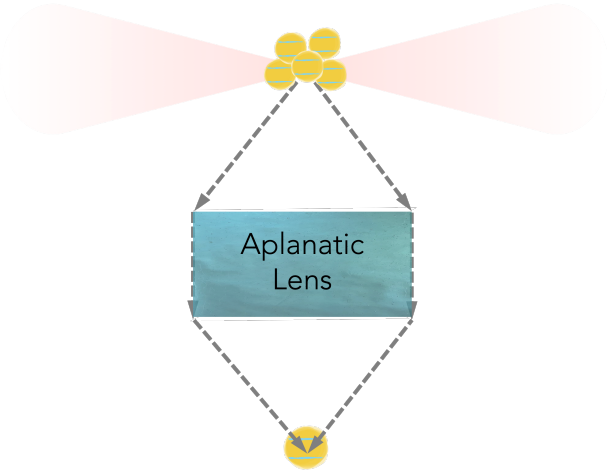

Figure 5.0.4: Schematic representation of the trap formed from lensed dipole-dipole forces. N atoms on the top are trapped by a tweezer at one of the focal points of the aplanatic lens system. The dipole-dipole forces between an atom placed around the other focal point of the lens and the collection of atoms on the top can be sufficiently strong to counteract gravity.

is the opposite. The functional form of H'_A is given by Eq. 3.0.27. In this way, if we only have one atom on each side (called A1 and A2), the interaction energy will be

$$\begin{aligned} H'_{A,\text{tot}} =& \hbar J_{12} \hat{\sigma}_+^{(A1)} \hat{\sigma}_-^{(A2)} + \hbar J_{21} \hat{\sigma}_+^{(A2)} \hat{\sigma}_-^{(A1)} \\ =& \hbar J_{12} \left[\hat{\sigma}_+^{(A1)} \hat{\sigma}_-^{(A2)} + \hat{\sigma}_+^{(A2)} \hat{\sigma}_-^{(A1)} \right]. \end{aligned} \tag{5.0.10}$$

The dipole-dipole trap will be given by the zone of minimum potential of the expectation value

$$\left\langle H'_{A,\text{tot}} \right\rangle = \hbar J_{12} \left\langle \hat{\sigma}_+^{(A1)} \hat{\sigma}_-^{(A2)} + \hat{\sigma}_+^{(A2)} \hat{\sigma}_-^{(A1)} \right\rangle. \tag{5.0.11}$$

In what follows, we will use the notation $\langle \hat{\sigma}_\pm \rangle \equiv \langle \sigma_\pm \rangle$, $\sigma_+\sigma_- = \rho_{ee}$, $\sigma_-\sigma_+ = \rho_{gg}$, and for convenience we write

$$\xi = \left\langle \hat{\sigma}_+^{(A1)} \hat{\sigma}_-^{(A2)} + \hat{\sigma}_+^{(A2)} \hat{\sigma}_-^{(A1)} \right\rangle. \tag{5.0.12}$$

In addition, we will make the approximation that atomic excitation is low enough that saturation can be neglected (we treat a factor $\rho_{gg} - \rho_{ee} \approx 1$), which also implies

that the dipoles are not correlated, i.e.,

$$\left\langle \sigma_+^{(A1)} \sigma_-^{(A2)} \right\rangle \approx \left\langle \sigma_+^{(A1)} \right\rangle \left\langle \sigma_-^{(A2)} \right\rangle . \tag{5.0.13}$$

To find the steady state, we can use the equation of motion for $\sigma_-^{(i)}$, given by Eq. 3.1.3 by replacing the Green's dyadic function found in the previous chapter, Eq. 4.2.3

$$\dot{\hat{\sigma}}_-^{(i)} = \left(\mathrm{i}\delta_D - \frac{\gamma_0}{2} \right) \hat{\sigma}_-^{(i)} + i\Omega + i\frac{\mu_0 \omega_D^2}{\hbar} \sum_j \mathbf{d}^\dagger \cdot \overleftrightarrow{\mathbf{G}}_{\mathrm{PSF}} \left(\mathbf{r}_i, \mathbf{r}_j \right) \cdot \mathbf{d} \; \hat{\sigma}_-^{(j)}. \tag{5.0.14}$$

For convenience, we will define

$$G_{12} \equiv J_{12} - \mathrm{i}\Gamma_{12}/2. \tag{5.0.15}$$

For our case of two atoms, we will obtain different steady states for atom A1 (which is under the effect of an external drive) and for atom A2:

$$\left\langle \sigma_-^{(A1)} \right\rangle = \frac{-\mathrm{i}\left(\Omega - G_{12} \left\langle \sigma_-^{(A2)} \right\rangle \right)}{-\mathrm{i}\delta_D - \gamma_0/2} \tag{5.0.16}$$

$$\left\langle \sigma_-^{(A2)} \right\rangle = \frac{-\mathrm{i}G_{12}\sigma_-^{(A1)}}{\gamma_0/2}. \tag{5.0.17}$$

where the detuning is given by $\delta_D = \omega_0 - \omega_D$. Solving the coupled equations we get

$$\left\langle \sigma_-^{(A1)} \right\rangle = \frac{-\mathrm{i}\Omega}{-\mathrm{i}\delta_D - \gamma_0/2 - 2/\gamma_0 G_{12}^2} \tag{5.0.18}$$

$$\left\langle \sigma_-^{(A2)} \right\rangle = \frac{2\Omega G_{12}/\gamma_0}{-\mathrm{i}\delta_D - \gamma_0/2 - 2/\gamma_0 G_{12}^2} \tag{5.0.19}$$

and the expressions for the probabilities

$$\rho_{ee}^{(A1)} = \frac{-i\Omega}{\gamma_0} \left[\left\langle \sigma_-^{(A1)} \right\rangle - \left\langle \sigma_+^{(A1)} \right\rangle \right] - \frac{i}{\gamma_0} \left[G_{12} \left\langle \sigma_+^{(A1)} \sigma_-^{(A2)} \right\rangle - G_{12}^* \left\langle \sigma_+^{(A2)} \sigma_-^{(A1)} \right\rangle \right] \tag{5.0.20}$$

$$\rho_{22}^{(A2)} = \frac{-i}{\gamma_0} \left[G_{12} \left\langle \sigma_+^{(A2)} \sigma_-^{(A1)} \right\rangle - G_{12}^* \left\langle \sigma_+^{(A1)} \sigma_-^{(A2)} \right\rangle \right]. \tag{5.0.21}$$

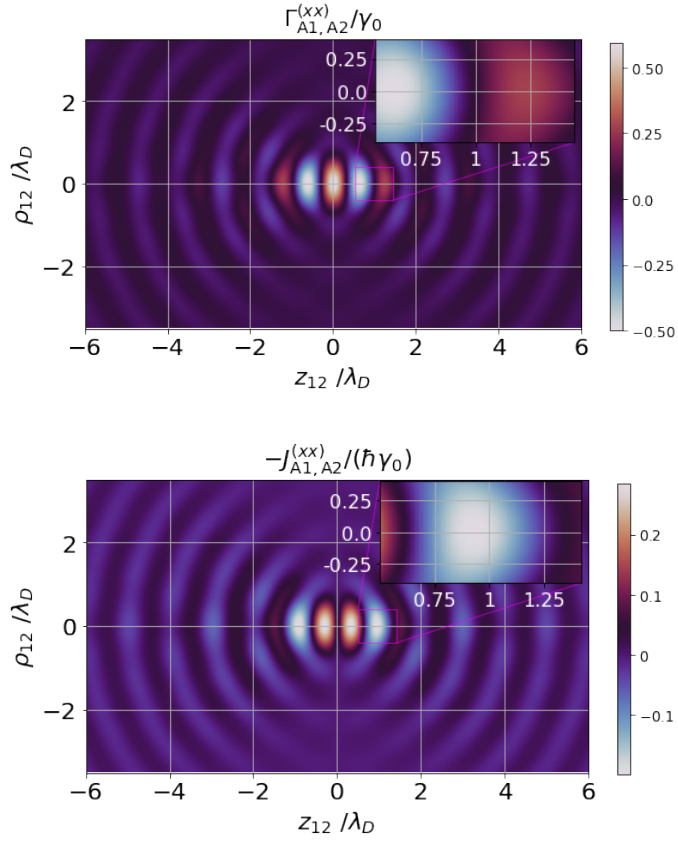

Figure 5.0.5: A closer look at the spatial dependence of dissipative and dispersive interactions, where the zone where the atomic trap will operate can be seen more clearly. Near the potential minimum, a low contribution of Γ_{12} is observed.

Fig. 5.0.5 shows an area where an atomic trap is expected, near $z_{12} \approx 0.92\lambda_D$. As we will see later, the lensing potential is modified by the gravitational potential, however there is enough depth to configure an atomic trap. Then, the expectation value of $\langle H'_{A,\text{tot}} \rangle$ coincides with the minimum of $\langle J_{12} \rangle \equiv J_{12}^{\min}$. For a lens with aperture $\theta_{\max} = \pi/3$, we obtain a subradiance given by $\langle \Gamma_{12} \rangle \equiv \Gamma_{12}^{\min} \approx -0.15\gamma_0$ and a level shift $J_{12}^{\min} \approx 0.4\gamma_0$.

We now analyze the effect of detuning on the atomic population and correlations, that determine the potential seen by A2. Defining $s = \left\langle \sigma_-^{(A1)} \right\rangle_0$ as the atomic state in Eq. 5.0.16 when there is no coupling between both atoms ($G_{12} = 0$), we can

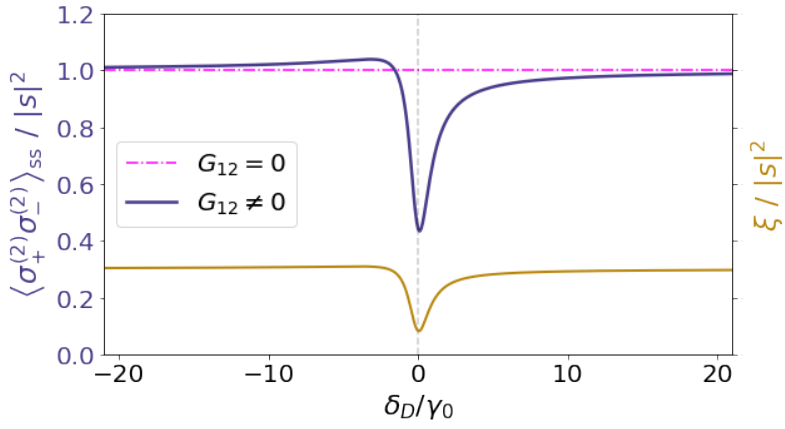

Figure 5.0.6: In violet: probability of finding excited atom A1 as δ_D varies, with optical drive only (dashed line) and a dipole-dipole interaction with atom A2 (solid line). The asymmetry in the peak of the latter is due to the non-zero contribution of G_{12}^2. In gold: sum of the correlations ξ. As can be seen from the shape of the graphs, there is a scale factor between ξ and $\left\langle \sigma_+^{(2)}\sigma_-^{(2)} \right\rangle_{\text{ss}}$, independent of the detuning δ_D.

obtain the saturation parameter for an atom subjected to an external drive,

$$|s|^2 = \left\langle \sigma_+^{(A1)} \right\rangle_0 \left\langle \sigma_-^{(A1)} \right\rangle_0 = \frac{\Omega^2}{\delta_D^2 + \gamma_0^2/4}. \tag{5.0.22}$$

To get $|s|^2$ constant, we have to adjust the intensity as δ_D changes setting the numerical value of the Rabi frequency

$$\Omega = |s|\sqrt{\delta_D^2 + \gamma_0^2/4}. \tag{5.0.23}$$

Equation 5.0.22 represents the probability of finding the excited atom A1 if we ignore the presence of A2, as can be seen in Fig. 5.0.6.

We can estimate the average lifetime t_{trap} of the alleged atomic trap for the non-driven atom A2 (that is not under the control of the optical tweezer) by comparing the depth of the potential well $\Delta U_{\text{pw}} = \Delta \left\langle H_A' \right\rangle_{\text{ss}}$ (see Fig. 5.0.7) with the heating rate of A2 due to spontaneous emission. Assuming that the atom gains recoil energy after every cycle of spontaneous emission, the heating rate is given by

$$R_{\text{heat,pw}}^{(2)} \approx \text{E}_\text{r} \times \Gamma_{\text{tot}} \left(z_{12}^{\min}\right) \times \left\langle \sigma_+^{(A2)}\sigma_-^{(A2)} \right\rangle_{\text{ss}}, \tag{5.0.24}$$

where $\mathrm{E_r} = \hbar^2 k_D^2/2m$ is the recoil energy and Γ_{tot} is the total atomic decay rate, which in our case it will suffice to say that it is slightly less than γ_0. The decorrelation approximation allows one to rewrite

$$R^{(2)}_{\mathrm{heat,pw}} \approx 4E_r\Gamma_{\mathrm{tot}} \left|G_2\right|^2 \gamma_0^{-2} \left\langle \sigma_+^{(A1)} \right\rangle \left\langle \sigma_-^{(A1)} \right\rangle \tag{5.0.25}$$

$$\Delta U_{\mathrm{pw}} \approx 4\Delta J_{12}\gamma_0^{-1} \,\mathrm{Im}\left\{G_{12}\right\} \left\langle \sigma_+^{(A1)} \right\rangle \left\langle \sigma_-^{(A1)} \right\rangle \tag{5.0.26}$$

where $\Delta J_{12} = J_{12}^{\mathrm{top}} - J_{12}^{\mathrm{min}}$ and J_{12}^{top} is the value of the energy shift at the top of the potential well. We obtain the detuning independent rate

$$\frac{\Delta U_{\mathrm{pw}}}{R^{(2)}_{\mathrm{heat,pw}}} = \frac{\Delta J_{12}}{E_r}\frac{\gamma_0}{\Gamma_{\mathrm{tot}}}\frac{\mathrm{Im}\, G_{12}}{\left|G_{12}\right|^2}, \tag{5.0.27}$$

Near z_{12}^{min} energy modifications dominate ($J_{12}^2 \gg \Gamma_{12}^2/4$), so the rate can be reduced to

$$\frac{\Delta U_{\mathrm{pw}}}{R^{(2)}_{\mathrm{heat,pw}}} \approx \frac{\hbar}{E_r}\frac{\gamma}{\Gamma_{\mathrm{tot}}}\frac{\mathrm{Im}\, G_{12}}{\mathrm{Re}\, G_{12}}\frac{\Delta J_{12}}{J_{12}}. \tag{5.0.28}$$

We now study the behavior of the trap in a realistic scenario with alkaline atoms. Let us consider ^{133}Cesium atoms in and their $6^2\,\mathrm{S}_{1/2} \longrightarrow 6^2\mathrm{P}_{3/2}$ transition as a two-level system, with dipole moment $\mathbf{d} = 2.69 \times 10^{-29}\mathrm{C}\cdot\mathrm{m}$, decay rate $\gamma_0 = 2\pi \cdot 5.23\mathrm{MHz}$, $\lambda_0 = 852\mathrm{nm}$ and $m = 1.66 \times 10^{-27}\mathrm{Kg}$ [37]. We can benefit from the detuning-independent relation in Eq. 5.0.27 using the optical tweezer that controls A1 as the external pump with $|\delta_D| \gg 1$, which means an advantage in the experimental setup. A2 is then confined only due to the resonant interaction with A1 mediated by an aplanatic lens of NA given by $\theta_{\mathrm{max}} = \pi/3$.

Figure 5.0.7 shows the trapping potential $\langle H'_A \rangle_{\mathrm{ss}} + U_g$, being U_g the gravitational potential for the atom with respect to $z_{12} = 0$, and heating rate as a function of the position along the optical axis. The external pump for A1 coincides with its red-detuned optical tweezer ($\delta_D \ll 1$). At position z_{12}^{min} a depression suitable for an atomic trap can be seen. The life time of the trap will not only depend on the difference between the bottom and the top of the well, $\Delta J_{12} = 0.9\hbar\Gamma_D$ for the

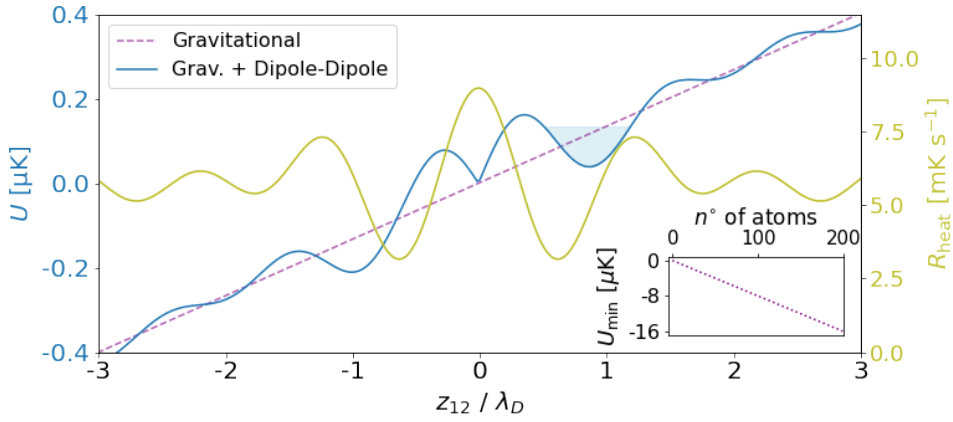

Figure 5.0.7: (b) In blue: comparison of potential energy from gravity and dipole-dipole interaction through a lens, evaluated in the steady state Eq. **??**. The reference for the gravitational potential energy is fixed at $z_{12} = 0$. In gold: scattering rate from the emission of photons, obtained via Eq. 5.0.24. The inset shows the minimum potential produced by the lensing field of $0 < N < 200$ atoms, which would lead to a trap powerful enough to control the mean position of an atom at the other end of the lens for thousands of cycles of spontaneous emission.

present configuration, but also on the comparison with the recoil energy E_{r},

$$t_{\mathrm{trap}} = \frac{\Delta U_{\mathrm{pw}} - E_{\mathrm{r}}}{R^{(2)}_{\mathrm{heat,pw}}}. \tag{5.0.29}$$

The shaded area shows the size of E_{r} compared to the potential well

$$\Delta U_{\mathrm{pw}} = \hbar \Delta J_{12} \xi. \tag{5.0.30}$$

Taking into consideration the presented configuration, equation 5.0.29 gives us a trapping time about

$$t_{\mathrm{trap}} \approx 1170 \gamma_0^{-1}. \tag{5.0.31}$$

Generalizing the modified interaction Hamiltonian H'_A to N_i atoms on the top of the optical system shown in Fig. 5.0.4,

$$H'_A = -\sum_i^{N_i} J^{\mathrm{R}}_{i,A2} \left(\hat{\sigma}^{(i)}_+ \hat{\sigma}^{(A2)}_- + \hat{\sigma}^{(A2)}_+ \hat{\sigma}^{(i)}_- \right), \tag{5.0.32}$$

we can consider a larger number of atoms at the upper focal point and thus obtain a linear increase in well depth with N_i.

$$t_{\text{trap}} \approx 1170 N_i \gamma_0^{-1}.. \tag{5.0.33}$$

The inset of Fig. 5.0.7 shows this increase. Although such scenario can greatly improve the effects of dipole-dipole interactions due to its collective nature, one would have to more carefuly consider Casimir interactions between near ground-state atoms as they start clumping together. However, the fact that we can neglect Casimir interactions between ground-state atoms (of the form $\rho_{gg}^{(i)}\rho_{gg}^{(i')}$), is argued since their spatial decay is very fast ($\sim 1/d^6$ in free space, d being the interatomic distance) [39].

A reliable and sustainable trap will require an external cooling mechanism before the heating rate dominates. This can be certainly done with external lasers or considering the effect in the atomic motion of red-detuned drive lasers. However, he we present a proof of principle of the mechanism that would make possible to restrict the mean position of alkali atoms using only the far-field resonant dipole-dipole interaction mediated by a large aperture aplanatic lens.

Chapter 6

Conclusions

In this work, the necessary elements to establish an atomic trap using only the dipole-dipole resonant interaction between distant atoms mediated by an aplanatic lens with both equal focal lengths were derived from its foundations.

Specifically, a lens with aperture $\theta_{\max} = \pi/3$ in a medium with refractive index $n \approx 1$ was used to collect part of the radiation emitted from an atomic group (whose position is controlled by a red-detuning optical tweezer) and focus it towards another group of atoms to induce control of the second group of atoms.

During the derivation of the expressions necessary to compare these long range interactions, alkali elements were assumed that under certain conditions can be treated as a two-level atom. For a specific analysis of the setup for this particular work, ^{133} Cesium atoms and their cyclic transition $|F = 4, m_F = \pm 4\rangle \longrightarrow |F' = 5, m_{F'} = \pm 5\rangle$ were used.

The research allowed us to conclude that it is possible to restrict and know the average position of a group of atoms for tens of thousands of periods of spontaneous emission. In addition to the purely intellectual interest that this atomic control of an indirect nature supposes, this montage opens up new possibilities in the field of CP interactions. Such a lens-mediated enhancement of the far-field resonant dipole-dipole interaction could be used to investigate the phenomenon of self-organization of a chain of atoms in the focal zone (for which the equations of motion of the quantum centers of mass are already derived and can be seen in the appendix 7.3,

being an important contribution of this work for future investigations) or the study of Casimir-Polder forces at a distance, a paradigmatic case of the state-of-the-art of forces between neutral particles.

Chapter 7

Appendices

7.1 Master Eq Calculus

In order to obtain the Born-Markov master equation for the atom density matrix evolution we have to expand each term of the expression

$$\begin{aligned}\frac{\mathrm{d}\rho_A}{\mathrm{d}t} = &- \underbrace{\frac{1}{\hbar^2}\,\mathrm{Tr}_F \int_0^\infty \mathrm{d}\tau H_{AF}(t) H_{AF}(t-\tau)\rho_A \otimes |0\rangle\langle 0|}_{\text{(I)}} \\ &- \underbrace{\frac{1}{\hbar^2}\,\mathrm{Tr}_F \int_0^\infty \mathrm{d}\tau \rho_A \otimes |0\rangle\langle 0| H_{AF}(t-\tau) H_{AF}(t)}_{\text{(II)}} \\ &+ \underbrace{\frac{1}{\hbar^2}\,\mathrm{Tr}_F \int_0^\infty \mathrm{d}\tau H_{AF}(t)\rho_A \otimes |0\rangle\langle 0| H_{AF}(t-\tau)}_{\text{(III)}} \\ &+ \underbrace{\frac{1}{\hbar^2}\,\mathrm{Tr}_F \int_0^\infty \mathrm{d}\tau H_{AF}(t-\tau)\rho_A \otimes |0\rangle\langle 0| H_{AF}(t)}_{\text{(IV)}}\,. \end{aligned} \tag{7.1.1}$$

To begin with, let us consider the first of them:

$$
\begin{aligned}
(\mathrm{I}) = -\frac{1}{\hbar^2}\,\mathrm{Tr}_F \int_0^\infty \mathrm{d}\tau \Bigg[\sum_{i=1}^{N} \int \mathrm{d}^3 r \int \mathrm{d}\omega \left(\hat{\sigma}_+^{(i)} e^{-i\delta_- t} \right) \mathbf{d}^\dagger \cdot \overleftrightarrow{\mathbf{G}}_e \left(\mathbf{r}_i, \mathbf{r}, \omega \right) \cdot \hat{\mathbf{f}}(\mathbf{r}, \omega) \\
+ \hat{\mathbf{f}}^\dagger(\mathbf{r}, \omega) \cdot \overleftrightarrow{\mathbf{G}}_e^{\,\dagger} \left(\mathbf{r}_i, \mathbf{r}, \omega \right) \cdot \mathbf{d} \left(\hat{\sigma}_-^{(i)} \mathrm{e}^{\mathrm{i}\delta_- t} \right) \Bigg] \times \qquad (7.1.2) \\
\Bigg[\sum_{j=1}^{N} \int \mathrm{d}^3 r' \int \mathrm{d}\omega' \left(\hat{\sigma}_+^{(j)} e^{-i\delta_- (t-\tau)} \right) \mathbf{d}^\dagger \cdot \overleftrightarrow{\mathbf{G}}_e \left(\mathbf{r}_j, \mathbf{r}', \omega' \right) \cdot \hat{\mathbf{f}}(\mathbf{r}', \omega') \\
+ \hat{\mathbf{f}}^\dagger(\mathbf{r}', \omega') \cdot \overleftrightarrow{\mathbf{G}}_e^{\,\dagger} \left(\mathbf{r}_j, \mathbf{r}', \omega' \right) \cdot \mathbf{d} \left(\hat{\sigma}_-^{(j)} \mathrm{e}^{\mathrm{i}\delta_- (t-\tau)} \right) \Bigg] \rho_A \otimes |\{0\}\rangle\langle\{0\}|
\end{aligned}
$$

Remembering that $\mathrm{Tr}_F\, A = \sum_k \langle k|A|k\rangle$, and expanding the square brackets

$$
\left[\overleftrightarrow{\mathbf{G}} \cdot \mathbf{f} + \mathbf{f}^\dagger \cdot \overleftrightarrow{\mathbf{G}}^\dagger \right] \left[\overleftrightarrow{\mathbf{G}} \cdot \mathbf{f} + \mathbf{f}^\dagger \cdot \overleftrightarrow{\mathbf{G}}^\dagger \right] = \overleftrightarrow{\mathbf{G}} \cdot \mathbf{f} \;\; \overleftrightarrow{\mathbf{G}} \cdot \mathbf{f} + \overleftrightarrow{\mathbf{G}} \cdot \mathbf{f}\, \mathbf{f}^\dagger \cdot \overleftrightarrow{\mathbf{G}}^\dagger + \mathbf{f}^\dagger \cdot \overleftrightarrow{\mathbf{G}}^\dagger \overleftrightarrow{\mathbf{G}} \cdot \mathbf{f} + \mathbf{f}^\dagger \cdot \overleftrightarrow{\mathbf{G}}^\dagger \;\; \mathbf{f}^\dagger \cdot \overleftrightarrow{\mathbf{G}}^\dagger \qquad (7.1.3)
$$

we can realize that, in this case, we keep the term $\overleftrightarrow{\mathbf{G}} \cdot \mathbf{f}\; \mathbf{f}^\dagger \cdot \overleftrightarrow{\mathbf{G}}^\dagger$ only. One further consideration is

$$
\langle \{0\}|\hat{\mathbf{f}}(\mathbf{r}, \omega) \hat{\mathbf{f}}^\dagger(\mathbf{r}', \omega')|\{0\}\rangle = \delta^3(\mathbf{r} - \mathbf{r}')\delta(\omega - \omega'), \qquad (7.1.4)
$$

so the term (I) reads

$$
\begin{aligned}
(\mathrm{I}) = & -\frac{1}{\hbar^2}\,\mathrm{Tr}_F \int_0^\infty \mathrm{d}\tau \sum_{i,j}^{N} \int \mathrm{d}^3 r \int \mathrm{d}^3 r' \int \omega \int \omega' \left(\hat{\sigma}_+^{(i)} e^{-i\delta_- t} \right) \\
& \mathbf{d}^\dagger \cdot \overleftrightarrow{\mathbf{G}} \left(\mathbf{r}_i, \mathbf{r}, \omega \right) \cdot \hat{\mathbf{f}}(\mathbf{r}, \omega) \cdot \hat{\mathbf{f}}^\dagger(\mathbf{r}', \omega') \cdot \overleftrightarrow{\mathbf{G}}^{\,\dagger} \left(\mathbf{r}_j, \mathbf{r}', \omega \right) \cdot \mathbf{d} \\
& \left(\hat{\sigma}_-^{(j)} \mathrm{e}^{\mathrm{i}\delta_- (t-\tau)} \right) \rho_A \otimes |\{0\}\rangle\langle\{0\}| \qquad (7.1.5) \\
= & -\frac{1}{\hbar^2} \int_0^\infty \mathrm{d}\tau \sum_{i,j}^{N} \int \mathrm{d}^3 r \int \mathrm{d}^3 r' \int \omega \int \omega' \; \mathbf{d}^\dagger \cdot \overleftrightarrow{\mathbf{G}} \left(\mathbf{r}_i, \mathbf{r}, \omega \right) \cdot \overleftrightarrow{\mathbf{G}}^{\,\dagger} \left(\mathbf{r}_i, \mathbf{r}', \omega' \right) \cdot \mathbf{d} \\
& \delta^3(\mathbf{r} - \mathbf{r}')\delta(\omega - \omega') \left(\hat{\sigma}_+^{(i)} e^{-i\delta_- t} \right) \left(\hat{\sigma}_-^{(j)} \mathrm{e}^{\mathrm{i}\delta_- (t-\tau)} \right) \rho_A \otimes |\{0\}\rangle\langle\{0\}| \\
= & -\frac{1}{\hbar^2} \int_0^\infty \mathrm{d}\tau \sum_{i,j}^{N} \int \mathrm{d}^3 r \int \omega \; \mathbf{d}^\dagger \cdot \overleftrightarrow{\mathbf{G}} \left(\mathbf{r}_i, \mathbf{r}, \omega \right) \cdot \overleftrightarrow{\mathbf{G}}^{\,\dagger} \left(\mathbf{r}_j, \mathbf{r}, \omega \right) \cdot \mathbf{d} \\
& \left(\hat{\sigma}_+^{(i)} e^{-i\delta_- t} \right) \left(\hat{\sigma}_-^{(j)} \mathrm{e}^{\mathrm{i}\delta_- (t-\tau)} \right) \rho_A \otimes |\{0\}\rangle\langle\{0\}| \qquad (7.1.6)
\end{aligned}
$$

Now, using the fluctuation-dissipation relation [36],

$$\int \mathrm{d}^3 r \;\; \overleftrightarrow{\mathbf{G}}_e \left(\mathbf{r}_1, \mathbf{r}, \omega\right) \cdot \overleftrightarrow{\mathbf{G}}_e^{\dagger} \left(\mathbf{r}_2, \mathbf{r}, \omega\right) = \frac{\hbar \mu_0 \omega^2}{\pi} \operatorname{Im} \overleftrightarrow{\mathbf{G}} \left(\mathbf{r}_1, \mathbf{r}_2, \omega\right) \tag{7.1.7}$$

and the rotating-wave approximation in which

$$\int_0^{\infty} \mathrm{d}\tau e^{-i\delta_+ \tau} = 0 \tag{7.1.8}$$

$$\int_0^{\infty} \mathrm{d}\tau e^{-i\delta_- \tau} = \pi \delta(\omega - \omega_0) - i\mathcal{P} \frac{1}{\omega - \omega_0} \tag{7.1.9}$$

where $\mathcal{P}$ denotes the Cauchy principal value, we arrive to:

$$\begin{aligned} (\mathrm{I}) = &- \frac{1}{\hbar^2} \frac{\hbar \mu_0}{\pi} \pi \sum_{i,j}^{N} \int \mathbf{d}\omega \; \omega^2 \delta(\omega - \omega_0) \; \hat{\sigma}_+^{(i)} \hat{\sigma}_-^{(j)} \; \mathbf{d}^{\dagger} \cdot \operatorname{Im} \overleftrightarrow{\mathbf{G}} \left(\mathbf{r}_i, \mathbf{r}_j, \omega\right) \cdot \mathbf{d} \; \rho_A \\ &+ i \frac{\mu_0}{\hbar \pi} \sum_{i,j}^{N} \mathcal{P} \int \mathbf{d}\omega \frac{\omega^2}{\omega - \omega_0} \hat{\sigma}_+^{(i)} \hat{\sigma}_-^{(j)} \; \mathbf{d}^{\dagger} \cdot \operatorname{Im} \overleftrightarrow{\mathbf{G}} \left(\mathbf{r}_i, \mathbf{r}_j, \omega\right) \cdot \mathbf{d} \; \rho_A \end{aligned} \tag{7.1.10}$$

which can be rewritten as

$$\begin{aligned} \Rightarrow (\mathrm{I}) = &- \frac{\mu_0 \omega_0^2}{\hbar} \sum_{i,j}^{N} \; \hat{\sigma}_+^{(i)} \hat{\sigma}_-^{(j)} \; \mathbf{d}^{\dagger} \cdot \operatorname{Im} \overleftrightarrow{\mathbf{G}} \left(\mathbf{r}_i, \mathbf{r}_j, \omega\right) \cdot \mathbf{d} \; \rho_A \\ &+ i \frac{\mu_0}{\hbar \pi} \sum_{i,j}^{N} \mathcal{P} \int \mathbf{d}\omega \frac{\omega^2}{\omega - \omega_0} \hat{\sigma}_+^{(i)} \hat{\sigma}_-^{(j)} \; \mathbf{d}^{\dagger} \cdot \operatorname{Im} \overleftrightarrow{\mathbf{G}} \left(\mathbf{r}_i, \mathbf{r}_j, \omega\right) \cdot \mathbf{d} \; \rho_A \end{aligned} \tag{7.1.11}$$

The imaginary part of the Green's function is related to the real part via the Kramers-Kronig relation [36, 41]:

$$\frac{1}{\pi} \mathcal{P} \int_{-\infty}^{\infty} \frac{\mathrm{d}\omega}{\omega - \omega_0} \omega^2 \operatorname{Im} \overleftrightarrow{\mathbf{G}} \left(\boldsymbol{r}_m, \boldsymbol{r}_n, \omega\right) = \omega_0^2 \operatorname{Re} \overleftrightarrow{\mathbf{G}} \left(\boldsymbol{r}_m, \boldsymbol{r}_n, \omega\right) \tag{7.1.12}$$

so we finally get a human-readable version of the first term

$$\begin{aligned}(\mathrm{I}) = &- \frac{\mu_0\omega_0^2}{\hbar}\sum_{i,j}^{N}\ \hat{\sigma}_+^{(i)}\hat{\sigma}_-^{(j)}\ \mathbf{d}^\dagger\cdot \mathrm{Im}\overset{\leftrightarrow}{\mathbf{G}}\left(\mathbf{r}_i,\mathbf{r}_j,\omega\right)\cdot\mathbf{d}\ \rho_A \\ &+ i\frac{\mu_0\omega_0^2}{\hbar}\sum_{i,j}^{N}\ \hat{\sigma}_+^{(i)}\hat{\sigma}_-^{(j)}\ \mathbf{d}^\dagger\cdot \mathrm{Re}\overset{\leftrightarrow}{\mathbf{G}}\left(\mathbf{r}_i,\mathbf{r}_j,\omega\right)\cdot\mathbf{d}\ \rho_A. \end{aligned} \tag{7.1.13}$$

This same procedure must be carried out for second factor,

$$\begin{aligned}(\mathrm{II}) &= -\frac{1}{\hbar^2}\,\mathrm{Tr}_F\int_0^\infty \mathrm{d}\tau\rho_A\otimes|\{0\}\rangle\langle\{0\}|H_{AF}(t-\tau)H_{AF}(t) \\ &= -\frac{1}{\hbar^2}\,\mathrm{Tr}_F\int_0^\infty \mathrm{d}\tau\rho_A\otimes|\{0\}\rangle\langle\{0\}| \\ &\quad\left[\sum_{i=1}^{N}\int \mathrm{d}^3r\int\mathrm{d}\omega\left(\hat{\sigma}_+^{(i)}e^{-i\delta_-(t-\tau)}\right)\mathbf{d}^\dagger\cdot\overset{\leftrightarrow}{\mathbf{G}}\left(\mathbf{r}_i,\mathbf{r},\omega\right)\cdot\hat{\mathbf{f}}(\mathbf{r},\omega)\right. \\ &\quad\left.+\hat{\mathbf{f}}^\dagger(\mathbf{r},\omega)\cdot\overset{\leftrightarrow}{\mathbf{G}}^\dagger\left(\mathbf{r}_i,\mathbf{r}',\omega\right)\cdot\mathbf{d}\left(\hat{\sigma}_-^{(i)}\mathrm{e}^{\mathrm{i}\delta_-(t-\tau)}\right)\right]\times \\ &\quad\left[\sum_{j=1}^{N}\int \mathrm{d}^3r\int\mathrm{d}\omega\left(\hat{\sigma}_+^{(j)}e^{-i\delta_-t}\right)\mathbf{d}^\dagger\cdot\overset{\leftrightarrow}{\mathbf{G}}\left(\mathbf{r}_j,\mathbf{r},\omega\right)\cdot\hat{\mathbf{f}}(\mathbf{r},\omega)\right. \\ &\quad\left.+\ \hat{\mathbf{f}}^\dagger(\mathbf{r},\omega)\cdot\overset{\leftrightarrow}{\mathbf{G}}^\dagger\left(\mathbf{r}_j,\mathbf{r},\omega\right)\cdot\mathbf{d}\left(\hat{\sigma}_-^{(j)}\mathrm{e}^{\mathrm{i}\delta_-t}\right)\right]. \end{aligned} \tag{7.1.14}$$

Using the same tools as described above, we get for the second term:

$$\begin{aligned}\Rightarrow(\mathrm{II}) &= -\frac{1}{\hbar^2}\frac{\hbar\mu_0}{\pi}\rho_A\sum_{i,j}^{N}\int\mathbf{d}\omega\ \omega^2\ \mathbf{d}^\dagger\cdot\mathrm{Im}\overset{\leftrightarrow}{\mathbf{G}}\left(\mathbf{r}_j,\mathbf{r}_i,\omega\right)\cdot\mathbf{d} \\ &\quad\times\left[\hat{\sigma}_+^{(i)}\hat{\sigma}_-^{(j)}\left(\int_0^\infty\mathrm{d}\tau\mathrm{e}^{\mathrm{i}\delta_-\tau}\right)\right] \end{aligned} \tag{7.1.15}$$

$$\begin{aligned} &= -\frac{\mu_0\omega_0^2}{\hbar}\rho_A\sum_{i,j}^{N}\ \hat{\sigma}_+^{(i)}\hat{\sigma}_-^{(j)}\ \mathbf{d}^\dagger\cdot\mathrm{Im}\overset{\leftrightarrow}{\mathbf{G}}\left(\mathbf{r}_i,\mathbf{r}_j,\omega\right)\cdot\mathbf{d} \\ &\quad - i\frac{\mu_0\omega_0^2}{\hbar}\rho_A\sum_{i,j}^{N}\ \hat{\sigma}_+^{(i)}\hat{\sigma}_-^{(j)}\ \mathbf{d}^\dagger\cdot\mathrm{Re}\overset{\leftrightarrow}{\mathbf{G}}\left(\mathbf{r}_i,\mathbf{r}_j,\omega\right)\cdot\mathbf{d}. \end{aligned} \tag{7.1.16}$$

The third part requires the adoption of a new measure. If we expand it, we see that

$$\begin{aligned}(\mathrm{III}) =&\frac{1}{\hbar^2}\,\mathrm{Tr}_F\int_0^\infty \mathrm{d}\tau H_{AF}(t)\rho_A\otimes|\{0\}\rangle\langle\{0\}|H_{AF}(t-\tau)\\ =&\frac{1}{\hbar^2}\,\mathrm{Tr}_F\int_0^\infty \mathrm{d}\tau\left[\sum_{i=1}^N\int \mathrm{d}^3r\int \mathrm{d}\omega\left(\hat\sigma_+^{(i)}e^{-i\delta_- t}\right)\mathbf{d}^\dagger\cdot\overleftrightarrow{\mathbf{G}}\,(\mathbf{r}_i,\mathbf{r},\omega)\cdot\hat{\mathbf{f}}(\mathbf{r},\omega)\right.\\ &\left.+\,\hat{\mathbf{f}}^\dagger(\mathbf{r},\omega)\cdot\overleftrightarrow{\mathbf{G}}^\dagger\,(\mathbf{r}_i,\mathbf{r},\omega)\cdot\mathbf{d}\left(\hat\sigma_-^{(i)}\mathrm{e}^{\mathrm{i}\delta_- t}\right)\right]\ \rho_A\otimes|\{0\}\rangle\langle\{0\}|\\ &\times\left[\sum_{j=1}^N\int \mathrm{d}^3r'\int \mathrm{d}\omega'\left(\hat\sigma_+^{(j)}e^{-i\delta_-(t-\tau)}\right)\mathbf{d}^\dagger\cdot\overleftrightarrow{\mathbf{G}}\,(\mathbf{r}_j,\mathbf{r}',\omega')\cdot\hat{\mathbf{f}}(\mathbf{r}',\omega')\right.\\ &\left.+\hat{\mathbf{f}}^\dagger(\mathbf{r}',\omega')\cdot\overleftrightarrow{\mathbf{G}}^\dagger\,(\mathbf{r}_j,\mathbf{r}',\omega')\cdot\mathbf{d}\left(\hat\sigma_-^{(j)}\mathrm{e}^{\mathrm{i}\delta_-(t-\tau)}\right)\right]\end{aligned}\tag{7.1.17}$$

But now, what end of the expansion Eq. 7.1.4 survive after taking the trace over the field? Although in the previous cases the braket $\langle\{0\}|\ \ |\{0\}\rangle$ worked, we see that now it is null:

$$\langle\{0\}|\ (\overleftrightarrow{\mathbf{G}}\cdot\underbrace{\mathbf{f}}_{0}+\overleftrightarrow{\mathbf{G}}^\dagger\cdot\underbrace{\mathbf{f}^\dagger}_{0})\ \rho_A\otimes|\{0\}\rangle\langle\{0\}|\ (\overleftrightarrow{\mathbf{G}}\cdot\mathbf{f}+\overleftrightarrow{\mathbf{G}}^\dagger\cdot\mathbf{f}^\dagger)\ |\{0\}\rangle=0\tag{7.1.18}$$

but the only non-zero contribution will be given by

$$\begin{aligned}\langle\{1\}|\ (\overleftrightarrow{\mathbf{G}}\cdot\mathbf{f}+\overleftrightarrow{\mathbf{G}}^\dagger\cdot\mathbf{f}^\dagger)\ \rho_A\otimes|\{0\}\rangle\langle\{0\}|\ (\overleftrightarrow{\mathbf{G}}\cdot\mathbf{f}+\overleftrightarrow{\mathbf{G}}^\dagger\cdot\mathbf{f}^\dagger)\ |\{1\}\rangle&\\ =\overleftrightarrow{\mathbf{G}}^\dagger\ \rho_A\ \overleftrightarrow{\mathbf{G}}\ \ \delta^3(\mathbf{r}-\mathbf{r}')\delta(\omega-\omega')&\end{aligned}\tag{7.1.19}$$

Then, considering the rotating-wave approximation and rewriting the delta function in terms of plane waves $\delta^3(r-r')=\int\mathbf{d}^3\mathbf{k}\frac{1}{(2\pi)^3}\mathrm{e}^{\mathrm{i}\mathbf{k}\cdot(r-r')}$, we have:

$$\begin{aligned}(\mathrm{III}) =\frac{1}{\hbar^2}\int_0^\infty \mathrm{d}\tau\sum_{i,j}^N\int \mathrm{d}^3r\int \mathrm{d}^3r'\int\omega\int\omega'\ \hat\sigma_-^{(i)}\hat\sigma_+^{(j)}\mathrm{e}^{\mathrm{i}\delta_-\tau}&\\ \times\,\delta^3(\mathbf{r}-\mathbf{r}')\delta(\omega-\omega')\ \mathbf{d}\cdot\overleftrightarrow{\mathbf{G}}^\dagger\,(\mathbf{r}_i,\mathbf{r},\omega)\,\rho_A\,\overleftrightarrow{\mathbf{G}}\,(\mathbf{r}_j,\mathbf{r}',\omega)\cdot\mathbf{d}^\dagger&\end{aligned}\tag{7.1.20}$$

which after expanding reads

$$\begin{aligned}(\text{III}) = &\int \mathbf{d}^3\mathbf{k} \int \mathbf{d}\omega \left[\int_0^\infty d\tau \mathrm{e}^{\mathrm{i}\delta_- \tau}\right] \left[\sum_i^N \int \mathbf{d}^3 r \frac{\mathrm{e}^{\mathbf{i}\mathbf{k}\cdot\mathbf{r}}}{\hbar(2\pi)^{3/2}} \hat{\sigma}_-^{(i)} \mathbf{d}\cdot \overleftrightarrow{\mathbf{G}}^\dagger (\mathbf{r}_i, \mathbf{r}, \omega)\right] \\ &\rho_A \left[\sum_j^N \int \mathbf{d}^3 r' \frac{\mathrm{e}^{\mathbf{i}\mathbf{k}\cdot\mathbf{r}'}}{\hbar(2\pi)^{3/2}} \hat{\sigma}_+^{(j)} \overleftrightarrow{\mathbf{G}} (\mathbf{r}_j, \mathbf{r}', \omega)\cdot \mathbf{d}^\dagger\right] \\ = &\pi \int \mathbf{d}^3\mathbf{k} \left[\sum_i^N \int \mathbf{d}^3 r \frac{\mathrm{e}^{\mathbf{i}\mathbf{k}\cdot\mathbf{r}}}{\hbar(2\pi)^{3/2}} \hat{\sigma}_-^{(i)} \mathbf{d}\cdot \overleftrightarrow{\mathbf{G}}^\dagger (\mathbf{r}_i, \mathbf{r}, \omega_0)\right] \rho_A \\ &\times \left[\sum_j^N \int \mathbf{d}^3 r' \frac{\mathrm{e}^{\mathbf{i}\mathbf{k}\cdot\mathbf{r}'}}{\hbar(2\pi)^{3/2}} \hat{\sigma}_+^{(j)} \overleftrightarrow{\mathbf{G}} (\mathbf{r}_j, \mathbf{r}', \omega_0)\cdot \mathbf{d}^\dagger\right] + \text{Principal Value}\end{aligned} \tag{7.1.21}$$

The last term of the RHS is the principal value that arises from $\int_0^\infty d\tau \mathrm{e}^{\mathrm{i}\delta_-\tau}$. Its explicit expression is dispensable, since the term (IV) can be written as

$$\begin{aligned}(\text{IV}) = &\frac{1}{\hbar^2} \mathrm{Tr}_F \int_0^\infty \mathrm{d}\tau H_{AF}(t-\tau)\rho_A \otimes |\{0\}\rangle\langle\{0\}| H_{AF}(t) \\ = &\pi \int \mathbf{d}^3\mathbf{k} \left[\sum_i^N \int \mathbf{d}^3 r \frac{\mathrm{e}^{\mathbf{i}\mathbf{k}\cdot\mathbf{r}}}{\hbar(2\pi)^{3/2}} \hat{\sigma}_-^{(i)} \mathbf{d}\cdot \overleftrightarrow{\mathbf{G}}^\dagger (\mathbf{r}_i, \mathbf{r}, \omega_0)\right] \rho_A \\ &\times \left[\sum_j^N \int \mathbf{d}^3 r' \frac{e^{-i\mathbf{k}\cdot\mathbf{r}'}}{\hbar(2\pi)^{3/2}} \hat{\sigma}_+^{(j)} \overleftrightarrow{\mathbf{G}} (\mathbf{r}_j, \mathbf{r}', \omega_0)\cdot \mathbf{d}^\dagger\right] - \text{Principal Value}\end{aligned} \tag{7.1.22}$$

with the sign of the principal value opposite to that of the term (III). Adding (I) + (II) + (III) + (IV) and defining (see Eq. 2.5.8 and Eq. 7.1.24):

$$\Gamma_{ij} = 2\left(\frac{\mu_0\omega_0^2}{\hbar}\right) \mathbf{d}^\dagger \cdot \mathrm{Im}\, \overleftrightarrow{\mathbf{G}} (\mathbf{r}_i, \mathbf{r}_j, \omega_0)\cdot \mathbf{d} \tag{7.1.23}$$

$$J_{ij} = -\left(\frac{\mu_0\omega_0^2}{\hbar}\right) \mathbf{d}^\dagger \cdot \mathrm{Re}\, \overleftrightarrow{\mathbf{G}} (\mathbf{r}_i, \mathbf{r}_j, \omega_0)\cdot \mathbf{d} \tag{7.1.24}$$

we can finally get our master equation

$$\begin{aligned}\dot{\rho}_A = &-\sum_{i,j}^{N}\frac{\Gamma_{ij}}{2}\hat{\sigma}_+^{(i)}\hat{\sigma}_-^{(j)}\rho_A - i\sum_{i,j}^{N}J_{ij}\hat{\sigma}_+^{(i)}\hat{\sigma}_-^{(j)}\ \rho_A \\ &-\rho_A\sum_{i,j}^{N}\frac{\Gamma_{ij}}{2}\hat{\sigma}_+^{(i)}\hat{\sigma}_-^{(j)} + i\rho_A\sum_{i,j}^{N}J_{ij}\hat{\sigma}_+^{(i)}\hat{\sigma}_-^{(j)} \\ &+\int \mathbf{d}^3\mathbf{k}\left[\sum_{i}^{N}\int \mathbf{d}^3r\frac{\mathrm{e}^{\mathbf{i}\mathbf{k}\cdot\mathbf{r}}}{2\pi\hbar}\hat{\sigma}_-^{(i)}\mathbf{d}\cdot\overleftrightarrow{\mathbf{G}}^{\dagger}(\mathbf{r}_i,\mathbf{r},\omega_0)\right]\ \rho_A \\ &\times\left[\sum_{j}^{N}\int \mathbf{d}^3r'\frac{e^{-i\mathbf{k}\cdot\mathbf{r}'}}{2\pi\hbar}\hat{\sigma}_+^{(j)}\ \overleftrightarrow{\mathbf{G}}(\mathbf{r}_j,\mathbf{r}',\omega_0)\cdot\mathbf{d}^{\dagger}\right].\end{aligned} \tag{7.1.25}$$

By ordering this expression we can arrive at the master equation, Eq. 3.0.26, where the coherent evolution is given by the modified atomic Hamiltonian Eq. 3.0.27 and where the dissipation of the system as a result of its interaction with the environment is determined by Eq. 3.0.28. However, an open quantum system can alternatively be described using the master equation [40]

$$\dot{\rho}_A = -\frac{i}{\hbar}\left(H_{\text{eff}}\rho_A - \rho_A H_{\text{eff}}^{\dagger}\right) + \mathcal{L}'(\rho_A) \tag{7.1.26}$$

where we defined the non-Hermitian Hamiltonian

$$\begin{aligned}H_{\text{eff}} &= \hbar\sum_{i,j}^{N}J_{ij}\hat{\sigma}_+^{(i)}\hat{\sigma}_-^{(j)} - i\hbar\sum_{i,j}^{N}\frac{\Gamma_{ij}}{2}\hat{\sigma}_+^{(i)}\hat{\sigma}_-^{(j)}, \\ &= -\mu_0\omega_0^2\sum_{i,j}^{N}\mathbf{d}^{\dagger}\cdot\overleftrightarrow{\mathbf{G}}(\mathbf{r}_i,\mathbf{r}_j)\cdot\mathbf{d}\ \hat{\sigma}_+^{(i)}\hat{\sigma}_-^{(j)},\end{aligned} \tag{7.1.27}$$

and the dissipation due to the reservoir as

$$\mathcal{L}'(\rho_A) = \mathcal{L}(\rho_A) + \frac{1}{2}\left\{\sum_{i,j}^{N}\Gamma_{ij}\hat{\sigma}_+^{(i)}\hat{\sigma}_-^{(j)}\ ,\ \rho_A\right\}. \tag{7.1.28}$$

Both approaches in the Schrodinger picture are equivalent, however it is more convenient for our purpose to work in the operator space, as developed in the main text.

7.2 Green's Function Calculus

The point spread function which gives us the dyadic Green's function for the aplanatic lens it is constructed through the expression in Eq. 4.0.11. In this appendix we will detail the calculations to obtain $\overleftrightarrow{\mathbf{G}}_{\mathrm{PSF}}$ from the far-field free-space Green function $\overleftrightarrow{\mathbf{G}}_{\mathrm{FF}}$, which can be written compactly as

$$\overleftrightarrow{\mathbf{G}}_{\mathrm{FF}}\left(\mathbf{r},0\right)=\frac{\exp(\mathrm{i}kr)}{4\pi r}\ \overleftrightarrow{\mathbf{g}}, \tag{7.2.1}$$

with

$$\overleftrightarrow{\mathbf{g}}=\begin{bmatrix} 1-\cos^2\phi\sin^2\theta & -\sin\phi\cos\phi\sin^2\theta & -\cos\phi\sin\theta\cos\theta \\ -\sin\phi\cos\phi\sin^2\theta & 1-\sin^2\phi\sin^2\theta & -\sin\phi\sin\theta\cos\theta \\ -\cos\phi\sin\theta\cos\theta & -\sin\phi\sin\theta\cos\theta & \sin^2\theta \end{bmatrix}. \tag{7.2.2}$$

For simplicity, let's work by components

$$\overleftrightarrow{\mathbf{g}}=\begin{bmatrix} g_{11} & g_{12} & g_{13} \\ g_{21} & g_{22} & g_{23} \\ g_{31} & g_{32} & g_{33} \end{bmatrix}. \tag{7.2.3}$$

In order to obtain a semi-analytical expression for the azimuthal integration, we can use the identities [43]

$$\int_0^{2\pi}\left\{\begin{array}{c}\sin n\phi\\ \cos n\phi\end{array}\right\}\mathrm{e}^{\mathrm{i}x\cos(\phi-\varphi)}d\phi=2\pi i^n J_n(x)\left\{\begin{array}{c}\sin n\varphi\\ \cos n\varphi\end{array}\right\}. \tag{7.2.4}$$

From now on, each component will be worked on separately, arriving at sums of integrals given by Eqs. 4.2.4-4.2.7:

- g_{11} :

$$\begin{aligned}\left(\overleftrightarrow{\mathbf{G}}_{\mathrm{PSF}}\right)_{11} &= \frac{\mathrm{i}k}{8\pi^2}\int_0^{\theta_{\max}}\int_0^{2\pi}\left(1-\cos^2\phi\sin^2\theta\right)\mathrm{e}^{\mathrm{i}kz\cos\theta}\mathrm{e}^{\mathrm{i}k\rho\sin\theta\cos(\phi-\varphi)}\sin\theta\mathrm{d}\phi\mathrm{d}\theta \\ &= \frac{\mathrm{i}k}{8\pi^2}\left[\int_0^{\theta_{\max}}2\pi J_0(k\rho\sin\theta)\sin\theta\ \mathrm{e}^{\mathrm{i}kz\cos\theta}\mathrm{d}\theta\right. \\ &\qquad -\int_0^{\theta_{\max}}\pi J_0(k\rho\sin\theta)\sin^3\theta\ \mathrm{e}^{\mathrm{i}kz\cos\theta}\mathrm{d}\theta \\ &\qquad \left.+\cos(2\varphi)\int_0^{\theta_{\max}}\pi J_2(k\rho\sin\theta)\sin^3\theta\ \mathrm{e}^{\mathrm{i}kz\cos\theta}\mathrm{d}\theta\right] \\ &= \frac{\mathrm{i}k}{8\pi}\left(I_1+I_2\cos(2\varphi)\right) \qquad (7.2.5)\end{aligned}$$

- g_{21} :

$$\begin{aligned}\left(\overleftrightarrow{\mathbf{G}}_{\mathrm{PSF}}\right)_{21} &= \frac{\mathrm{i}k}{8\pi^2}\int_0^{\theta_{\max}}\int_0^{2\pi}\left(-\sin\phi\cos\phi\sin^2\theta\right)\mathrm{e}^{\mathrm{i}kz\cos\theta}\mathrm{e}^{\mathrm{i}k\rho\sin\theta\cos(\phi-\varphi)}\sin\theta\mathrm{d}\phi\mathrm{d}\theta \\ &= \frac{\mathrm{i}k}{8\pi^2}\int_0^{\theta_{\max}}\sin^3\theta\left(\pi J_2(k\rho\sin\theta)\sin(2\varphi)\right)\ \mathrm{e}^{\mathrm{i}kz\cos\theta}\mathrm{d}\theta \\ &= \frac{\mathrm{i}k}{8\pi}I_2\sin(2\varphi) \qquad (7.2.6)\end{aligned}$$

- g_{31} :

$$\begin{aligned}\left(\overleftrightarrow{\mathbf{G}}_{\mathrm{PSF}}\right)_{31} &= \frac{\mathrm{i}k}{8\pi^2}\int_0^{\theta_{\max}}\int_0^{2\pi}\left(-\cos\phi\sin\theta\cos\theta\right)\mathrm{e}^{\mathrm{i}kz\cos\theta}\mathrm{e}^{\mathrm{i}k\rho\sin\theta\cos(\phi-\varphi)}\sin\theta\mathrm{d}\phi\mathrm{d}\theta \\ &= \frac{\mathrm{i}k}{8\pi^2}\int_0^{\theta_{\max}}\left(-2\pi\mathrm{i}J_1(k\rho\sin\theta)\cos(\varphi)\right)\sin^2\theta\cos\theta\ \mathrm{e}^{\mathrm{i}kz\cos\theta}\mathrm{d}\theta \\ &= \frac{\mathrm{i}k}{8\pi}\left(-2\mathrm{i}I_3\cos(\varphi)\right) \qquad (7.2.7)\end{aligned}$$

- g_{12} :

$$\left(\overleftrightarrow{\mathbf{G}}_{\mathrm{PSF}}\right)_{21} = \left(\overleftrightarrow{\mathbf{G}}_{\mathrm{PSF}}\right)_{12} \qquad (7.2.8)$$

- g_{22} :

$$\begin{aligned}\left(\overleftrightarrow{\mathbf{G}}_{\mathrm{PSF}}\right)_{22} &= \frac{\mathrm{i}k}{8\pi^2}\int_0^{\theta_{\max}}\int_0^{2\pi}\left(1-\sin^2\phi\sin^2\theta\right)\mathrm{e}^{\mathrm{i}kz\cos\theta}\mathrm{e}^{\mathrm{i}k\rho\sin\theta\cos(\phi-\varphi)}\sin\theta\mathrm{d}\phi\mathrm{d}\theta \\ &= \frac{\mathrm{i}k}{8\pi^2}\left[\int_0^{\theta_{\max}}2\pi J_0(k\rho\sin\theta)\sin\theta\ \mathrm{e}^{\mathrm{i}kz\cos\theta}\mathrm{d}\theta\right. \\ &\qquad -\int_0^{\theta_{\max}}\pi J_0(k\rho\sin\theta)\sin^3\theta\ \mathrm{e}^{\mathrm{i}kz\cos\theta}\mathrm{d}\theta \\ &\qquad \left.-\cos(2\varphi)\int_0^{\theta_{\max}}\pi J_2(k\rho\sin\theta)\sin^3\theta\ \mathrm{e}^{\mathrm{i}kz\cos\theta}\mathrm{d}\theta\right] \\ &= \frac{\mathrm{i}k}{8\pi}\big(I_1-I_2\cos(2\varphi)\big) \qquad (7.2.9)\end{aligned}$$

- g_{32} :

$$\begin{aligned}\left(\overleftrightarrow{\mathbf{G}}_{\mathrm{PSF}}\right)_{32} &= \frac{\mathrm{i}k}{8\pi^2}\int_0^{\theta_{\max}}\int_0^{2\pi}\left(-\sin\phi\sin\theta\cos\theta\right)\mathrm{e}^{\mathrm{i}kz\cos\theta}\mathrm{e}^{\mathrm{i}k\rho\sin\theta\cos(\phi-\varphi)}\sin\theta\mathrm{d}\phi\mathrm{d}\theta \\ &= \frac{\mathrm{i}k}{8\pi^2}\int_0^{\theta_{\max}}\left(-2\pi\mathrm{i}J_1(k\rho\sin\theta)\sin(\varphi)\right)\sin^2\theta\cos\theta\mathrm{e}^{\mathrm{i}kz\cos\theta}\mathrm{d}\theta \\ &= \frac{\mathrm{i}k}{8\pi}\big(-2\mathrm{i}I_3\sin(\varphi)\big) \qquad (7.2.10)\end{aligned}$$

- g_{13} :

$$\left(\overleftrightarrow{\mathbf{G}}_{\mathrm{PSF}}\right)_{13} = \left(\overleftrightarrow{\mathbf{G}}_{\mathrm{PSF}}\right)_{31} \qquad (7.2.11)$$

- g_{23} :

$$\left(\overleftrightarrow{\mathbf{G}}_{\mathrm{PSF}}\right)_{23} = \left(\overleftrightarrow{\mathbf{G}}_{\mathrm{PSF}}\right)_{32} \qquad (7.2.12)$$

- g_{33} :

$$\begin{aligned}\left(\overleftrightarrow{\mathbf{G}}_{\mathrm{PSF}}\right)_{33} &= \frac{\mathrm{i}k}{8\pi^2}\int_0^{\theta_{\max}}\int_0^{2\pi}\left(\sin^2\theta\right)\mathrm{e}^{\mathrm{i}kz\cos\theta}\mathrm{e}^{\mathrm{i}k\rho\sin\theta\cos(\phi-\varphi)}\sin\theta\mathrm{d}\phi\mathrm{d}\theta \\ &= \frac{\mathrm{i}k}{8\pi^2}\int_0^{\theta_{\max}}\left(2\pi\mathrm{i}J_0(k\rho\sin\theta)\right)\sin^3\theta\mathrm{e}^{\mathrm{i}kz\cos\theta}\mathrm{d}\theta \\ &= \frac{\mathrm{i}k}{8\pi}\left(2I_4\right) \qquad (7.2.13)\end{aligned}$$

In this way, the matrix $\overleftrightarrow{\mathbf{G}}_{\mathrm{PSF}}$ written in the main text, Eq. 4.0.14. This expression takes its final form in Eq. 4.2.3, together with the integrals given by Eqs. 4.2.4-4.2.7.

7.3 Quantum Center of Mass Motion

Once the potential trap is effective in constraining the position of the atoms, it is possible to replace $X = p^x, p^y, p^z$ into Eq. 3.1.3 (with the point spread function $\overleftrightarrow{\mathbf{G}}_{\mathrm{PSF}}$ as the Green's function) to get the quantum center of mass motion for each atom. Without going into the laborious details, these equations of motion are given by

$$\dot{p}_z^i = -\hbar k_D\sum_j^{N_j}\Gamma_z(\mathbf{r}_i,\mathbf{r}_j,\omega_D)\,\mathrm{sgn}(z_i-z_j)\sigma_-^{(i)}\sigma_+^{(j)} \qquad (7.3.1)$$

$$\dot{p}_x^i = -\hbar k_D\sum_j^{N_j}\Gamma_x(\mathbf{r}_i,\mathbf{r}_j,\omega_D)\,\mathrm{sgn}(x_i-x_j)\sigma_-^{(i)}\sigma_+^{(j)} \qquad (7.3.2)$$

$$\dot{p}_y^i = -\hbar k_D\sum_j^{N_j}\Gamma_y(\mathbf{r}_i,\mathbf{r}_j,\omega_D)\,\mathrm{sgn}(y_i-y_j)\sigma_-^{(i)}\sigma_+^{(j)} \qquad (7.3.3)$$

where the Γ-like functions are given by

$$\Gamma_z(\mathbf{r}_i,\mathbf{r}_j,\omega_D) = 2\frac{\mu_0\omega_0^2}{\hbar}\mathbf{d}^\dagger\cdot\mathrm{Im}\,\mathbf{G}_z(\mathbf{r}_i,\mathbf{r}_j,\omega_D)\cdot\mathbf{d} \qquad (7.3.4)$$

$$\Gamma_x(\mathbf{r}_i,\mathbf{r}_j,\omega_D) = 2\frac{\mu_0\omega_0^2}{\hbar}\mathbf{d}^\dagger\cdot\mathrm{Im}\,\mathbf{G}_x(\mathbf{r}_i,\mathbf{r}_j,\omega_D)\cdot\mathbf{d} \qquad (7.3.5)$$

$$\Gamma_y(\mathbf{r}_i,\mathbf{r}_j,\omega_D) = 2\frac{\mu_0\omega_0^2}{\hbar}\mathbf{d}^\dagger\cdot\mathrm{Im}\,\mathbf{G}_y(\mathbf{r}_i,\mathbf{r}_j,\omega_D)\cdot\mathbf{d} \qquad (7.3.6)$$

and are constructed from the matrices

$$\mathbf{G}_z(\mathbf{r}_i,\mathbf{r}_j,\omega_D)=\frac{\mathrm{i}k_D}{8\pi}\begin{bmatrix} I_{||1}+I_{||2}\cos(2\varphi_{ij}) & I_{||2}\sin(2\varphi_{ij}) & -2\mathrm{i}I_{||3}\cos\varphi_{ij} \\ I_{||2}\sin(2\varphi_{ij}) & I_{||1}-I_{||2}\cos(2\varphi_{ij}) & -2\mathrm{i}I_{||3}\sin\varphi_{ij} \\ -2\mathrm{i}I_{||3}\cos\varphi_{ij} & -2\mathrm{i}I_{||3}\sin\varphi_{ij} & 2I_{||4} \end{bmatrix} \tag{7.3.7}$$

$$\mathbf{G}_x(\mathbf{r}_i,\mathbf{r}_j,\omega_D)=\frac{\mathrm{i}k_D}{8\pi}\times \tag{7.3.8}$$

$$\begin{bmatrix} I^a_{\perp 1}\cos(\varphi_{ij})+I^b_{\perp 2}\cos(3\varphi_{ij}) & -I^a_{\perp 2}\sin(\varphi_{ij})+I^b_{\perp 2}\sin(3\varphi_{ij}) & -2iI^a_{\perp 3}\cos(2\varphi_{ij})+2iI^b_{\perp 3} \\ -I^a_{\perp 2}\sin(\varphi_{ij})+I^b_{\perp 2}\sin(3\varphi_{ij}) & I^b_{\perp 1}\cos(\varphi_{ij})-I^b_{\perp 2}\cos(3\varphi_{ij}) & -2iI^a_{\perp 3}\sin(2\varphi_{ij}) \\ -2iI^a_{\perp 3}\cos(2\varphi_{ij})+2iI^b_{\perp 3} & -2iI^a_{\perp 3}\sin(2\varphi_{ij}) & 4I_{\perp 4}\cos(\varphi_{ij}) \end{bmatrix} \tag{7.3.9}$$

$$\mathbf{G}_y(r_i,r_j)=\frac{\mathrm{i}k}{8\pi}\times \tag{7.3.10}$$

$$\begin{bmatrix} I^b_{\perp 1}\sin(\varphi_{ij})+I^b_{\perp 2}\sin(3\varphi_{ij}) & -I^a_{\perp 2}\cos(\varphi_{ij})-I^b_{\perp 2}\cos(3\varphi_{ij}) & -2iI^a_{\perp 3}\sin(2\varphi_{ij}) \\ -I^a_{\perp 2}\cos(\varphi_{ij})-I^b_{\perp 2}\cos(3\varphi_{ij}) & I^a_{\perp 1}\sin(\varphi_{ij})-I^b_{\perp 2}\sin(3\varphi_{ij}) & 2iI^a_{\perp 3}\cos(2\varphi_{ij})+2iI^b_{\perp 3} \\ -2iI^a_{\perp 3}\sin(2\varphi_{ij}) & 2iI^a_{\perp 3}\cos(2\varphi_{ij})+2iI^b_{\perp 3} & 4I_{\perp 4}\sin(\varphi_{ij}) \end{bmatrix} \tag{7.3.11}$$

whose matrix elements are linear combinations of the integrals

$$I_{||1} = \int_0^{\theta_{\max}} \cos\theta\sin\theta\{1+\cos^2\theta\}\mathrm{e}^{\mathrm{i}k_z|z_{ij}|}J_0(k\sin\theta\rho_{ij})\mathrm{d}\theta \tag{7.3.12}$$

$$I_{||2} = \int_0^{\theta_{\max}} \cos\theta\sin\theta\{1-\cos^2\theta\}\mathrm{e}^{\mathrm{i}k_z|z_{ij}|}J_2(k\sin\theta\rho_{ij})\mathrm{d}\theta \tag{7.3.13}$$

$$I_{||3} = \int_0^{\theta_{\max}} \cos\theta\sin^2\theta\cos\theta\mathrm{e}^{\mathrm{i}k_z|z_{ij}|}J_1(k\sin\theta\rho_{ij})\mathrm{d}\theta \tag{7.3.14}$$

$$I_{||4} = \int_0^{\theta_{\max}} \cos\theta\sin^3\theta\mathrm{e}^{\mathrm{i}k_z|z_{ij}|}J_0(k\sin\theta\rho_{ij})\mathrm{d}\theta \tag{7.3.15}$$

$$I^a_{\perp 1} = \int_0^{\theta_{max}} \sin^2\theta \left\{1 + 3\cos^2\theta\right\} \mathrm{e}^{\mathrm{i}k_z|z_{ij}|} J_1(k\sin\theta\rho_{ij})\mathrm{d}\theta \tag{7.3.16}$$

$$I^b_{\perp 1} = \int_0^{\theta_{max}} \sin^2\theta \left\{3 + \cos^2\theta\right\} \mathrm{e}^{\mathrm{i}k_z|z_{ij}|} J_1(k\sin\theta\rho_{ij})\mathrm{d}\theta \tag{7.3.17}$$

$$I^a_{\perp 2} = \int_0^{\theta_{max}} \sin^2\theta \left\{1 - \cos^2\theta\right\} \mathrm{e}^{\mathrm{i}k_z|z_{ij}|} J_1(k\sin\theta\rho_{ij})\mathrm{d}\theta \tag{7.3.18}$$

$$I^b_{\perp 2} = \int_0^{\theta_{max}} \sin^2\theta \left\{1 - \cos^2\theta\right\} \mathrm{e}^{\mathrm{i}k_z|z_{ij}|} J_3(k\sin\theta\rho_{ij})\mathrm{d}\theta \tag{7.3.19}$$

$$I^a_{\perp 3} = \int_0^{\theta_{max}} \sin^3\theta\cos\theta \mathrm{e}^{\mathrm{i}k_z|z_{ij}|} J_2(k\sin\theta\rho_{ij})\mathrm{d}\theta \tag{7.3.20}$$

$$I^b_{\perp 3} = \int_0^{\theta_{max}} \sin^3\theta\cos\theta \mathrm{e}^{\mathrm{i}k_z|z_{ij}|} J_0(k\sin\theta\rho_{ij})\mathrm{d}\theta \tag{7.3.21}$$

$$I_{\perp 4} = \int_0^{\theta_{max}} \sin^4\theta \mathrm{e}^{\mathrm{i}k_z|z_{ij}|} J_1(k\sin\theta\rho_{ij})\mathrm{d}\theta. \tag{7.3.22}$$

Referencias

[1] P. W. Milonni, *The Quantum Vacuum*. 1993.

[2] H. B. G. Casimir, "On the Attraction Between Two Perfectly Conducting Plates," *Indag. Math.*, vol. 10, pp. 261–263, 1948.

[3] H. B. G. Casimir and D. Polder, "The influence of retardation on the london-van der waals forces," *Phys. Rev.*, vol. 73, pp. 360–372, Feb 1948.

[4] D. E. Chang, K. Sinha, J. M. Taylor, and H. J. Kimble, "Trapping atoms using nanoscale quantum vacuum forces," *Nature Communications*, vol. 5, no. 1, p. 4343, 2014.

[5] D. A. T. Somers and J. N. Munday, "Conditions for repulsive casimir forces between identical birefringent materials," *Phys. Rev. A*, vol. 95, p. 022509, Feb 2017.

[6] F. S. S. Rosa, D. A. R. Dalvit, and P. W. Milonni, "Casimir interactions for anisotropic magnetodielectric metamaterials," *Phys. Rev. A*, vol. 78, p. 032117, Sep 2008.

[7] J. H. Wilson, A. A. Allocca, and V. Galitski, "Repulsive casimir force between weyl semimetals," *Phys. Rev. B*, vol. 91, p. 235115, Jun 2015.

[8] P. Rodriguez-Lopez and A. G. Grushin, "Repulsive casimir effect with chern insulators," *Phys. Rev. Lett.*, vol. 112, p. 056804, Feb 2014.

[9] M. Ishikawa, N. Inui, M. Ichikawa, and K. Miura, "Repulsive casimir force in liquid," *Journal of the Physical Society of Japan*, vol. 80, no. 11, p. 114601, 2011.

[10] M. Levin, A. P. McCauley, A. W. Rodriguez, M. T. H. Reid, and S. G. Johnson, "Casimir repulsion between metallic objects in vacuum," *Phys. Rev. Lett.*, vol. 105, p. 090403, Aug 2010.

[11] K. Sinha, "Repulsive vacuum-induced forces on a magnetic particle," *Phys. Rev. A*, vol. 97, p. 032513, Mar 2018.

[12] C. Henkel, K. Joulain, J.-P. Mulet, and J.-J. Greffet, "Radiation forces on small particles in thermal near fields," *Journal of Optics A: Pure and Applied Optics*, vol. 4, pp. S109–S114, aug 2002.

[13] K. Sinha, B. P. Venkatesh, and P. Meystre, "Collective effects in casimir-polder forces," *Phys. Rev. Lett.*, vol. 121, p. 183605, Nov 2018.

[14] E. Haller, J. Hudson, A. Kelly, D. A. Cotta, B. Peaudecerf, G. D. Bruce, and S. Kuhr, "Single-atom imaging of fermions in a quantum-gas microscope," *Nature Physics*, vol. 11, p. 738, 2015.

[15] A. Kaufman and K.-K. Ni, "Quantum science with optical tweezer arrays of ultracold atoms and molecules," *Nature Physics*, vol. 17, p. 1324, 2021.

[16] A. Asenjo-Garcia, M. Moreno-Cardoner, A. Albrecht, H. J. Kimble, and D. E. Chang, "Exponential improvement in photon storage fidelities using subradiance and "selective radiance" in atomic arrays," *Phys. Rev. X*, vol. 7, p. 031024, 2017.

[17] Y.-S. Chin, M. Steiner, and C. Kurtsiefer, "Nonlinear photon-atom coupling with 4pi microscopy," *Nature Communications*, vol. 8, p. 1200, 2017.

[18] L. C. Bianchet, N. Alves, L. Zarraoa, N. Bruno, and M. W. Mitchell, "Manipulating and measuring single atoms in the maltese cross geometry," 2021.

[19] S. G. B. O. e. a. Heller, I., "Sted nanoscopy combined with optical tweezers reveals protein dynamics on densely covered dna," *Nature Methods*, vol. 10, pp. 910–916, 2013.

[20] C. Robens, S. Brakhane, W. Alt, F. Kleißler, D. Meschede, G. Moon, G. Ramola, and A. Alberti, "High numerical aperture (na=0.92) objective lens

for imaging and addressing of cold atoms," *Opt. Lett.*, vol. 42, pp. 1043–1046, Mar 2017.

[21] P. Solano, P. Barberis-Blostein, F. K. Fatemi, L. A. Orozco, and S. L. Rolston, "Super-radiance reveals infinite-range dipole interactions through a nanofiber," *Nat. Commun.*, vol. 8, p. 1857, 2017.

[22] K. Sinha, P. Meystre, E. Goldschmidt, F. K. Fatemi, S. L. Rolson, and P. Solano, "Non-markovian collective emission from macroscopically separated emitters," *Phys. Rev. Lett.*, vol. 124, p. 043603, 2020.

[23] K. Sinha, P. Meystre, and P. Solano, "Non-markovian dynamics of collective atomic states coupled to a waveguide," *Nanophotonic Materials, Devices, and Systems*, vol. 11091, pp. 53 – 59, 2019.

[24] P. Solano, P. Barberis-Blostein, and K. Sinha, "Collective directional emission from distant emitters in waveguide qed," 2021.

[25] J. Enderlein, "Theoretical study of detection of a dipole emitter through an objective with high numerical aperture," *Opt. Lett.*, vol. 25, pp. 634–636, 2000.

[26] L. Mandel and E. Wolf, *Optical Coherence and Quantum Optics*. Cambridge University Press, 1995.

[27] J. D. Jackson, *Classical Electrodynamics, 2nd edn.* Wiley, 1975.

[28] L. Novotny and B. Hecht, *Principles of nano-optics*. Cambridge University Press, 2012.

[29] L. Barron and C. G. Gray, "The multipole interaction Hamiltonian for time dependent fields," *J. Phys. A*, vol. 6, pp. 50–61, 1973.

[30] E. M. Purcell, "Spontaneous emission probabilities at radio frequencies," *Phys. Rev.*, vol. 69, p. 681, 1946.

[31] K. H. Drexhage, M. Fleck, F. P. Schäfer, and W. Sperling, "Beeinflussung der Fluoreszenz eines Europium-chelates durch einen Spiegel," *Ber. Bunsenges. Phys. Chem.*, vol. 20, p. 1176, 1966.

[32] P. Goy, J. M. Raimond, M. Gross, and S. Haroche, "Observation of cavity-enhanced single-atom spontaneous emission," *Phys. Rev. Lett.*, vol. 50, p. 1903–1906, 1983.

[33] D. Kleppner, "Inhibited spontaneous emission," *Phys. Rev. Lett.*, vol. 47, p. 233–236, 1981.

[34] E. Yablonovitch, "Inhibited spontaneous emission in solid-state physics and electronics," *Phys. Rev. Lett.*, vol. 58, p. 2059–2062, 1987.

[35] S. Kühn, U. Hakanson, L. Rogobete, and V. Sandoghdar, "Enhancement of single molecule fluorescence using a gold nanoparticle as an optical nanoantenna," *Phys. Rev. Lett.*, vol. 97, p. 017402, 2006.

[36] S. Y. Buhmann, *Dispersion Forces II*. Springer-Verlag, 2012.

[37] D. A. Steck, *Cesium D Line Data*. available online at http://steck.us/alkalidata (revision 2.2.1, 21 November 2019).

[38] P. Meystre and M. Sargent, *Elements of Quantum Optics, 4th edn.* Springer-Verlag, 2007.

[39] S. Y. Buhmann, *Dispersion Forces I*. Springer-Verlag Berlin Heidelberg, 2012.

[40] H. P. Breuer and F. Petruccione, *The Theory of Open Quantum Systems*. Oxford University Press, 2002.

[41] S. Hassani, *Mathematical Physics*. Springer, 2013.

[42] F. Pedrotti, L. S. Pedrotti, and L. M. Pedrotti, *Introduction to Optics*. Pearson Education, 2006.

[43] U. Hohenester, *Nano and Quantum Optics*. Springer, 2020.

[44] R. Grimm, M. Weidemüller, and Y. B. Ovchinnikov, "Optical dipole traps for neutral atoms," vol. 42 of *Advances In Atomic, Molecular, and Optical Physics*, pp. 95–170, Academic Press, 2000.

[45] K. Sinha, A. González-Tudela, Y. Lu, and P. Solano, "Collective radiation from distant emitters," *Phys. Rev. A*, vol. 102, p. 043718, Oct 2020.